Published in "Journal of Comparative Neurology 523(18): 2637–2664, 2015"
which should be cited to refer to this work.

Neuropeptide F Neurons Modulate Sugar Reward During Associative Olfactory Learning of *Drosophila* Larvae

Astrid Rohwedder,[1] Mareike Selcho,[2] Bérénice Chassot,[1] and Andreas S. Thum[1,3,4]*

[1]Department of Biology, University of Fribourg, Fribourg, Switzerland
[2]Department of Neurobiology and Genetics, Theodor-Boveri-Institute, Biocenter, University of Würzburg, Würzburg, Germany
[3]Department of Biology, University of Konstanz, Konstanz, Germany
[4]Zukunftskolleg, University of Konstanz, Konstanz, Germany

ABSTRACT

All organisms continuously have to adapt their behavior according to changes in the environment in order to survive. Experience-driven changes in behavior are usually mediated and maintained by modifications in signaling within defined brain circuits. Given the simplicity of the larval brain of *Drosophila* and its experimental accessibility on the genetic and behavioral level, we analyzed if *Drosophila* neuropeptide F (dNPF) neurons are involved in classical olfactory conditioning. dNPF is an ortholog of the mammalian neuropeptide Y, a highly conserved neuromodulator that stimulates food-seeking behavior. We provide a comprehensive anatomical analysis of the dNPF neurons on the single-cell level. We demonstrate that artificial activation of dNPF neurons inhibits appetitive olfactory learning by modulating the sugar reward signal during acquisition. No effect is detectable for the retrieval of an established appetitive olfactory memory. The modulatory effect is based on the joint action of three distinct cell types that, if tested on the single-cell level, inhibit and invert the conditioned behavior. Taken together, our work describes anatomically and functionally a new part of the sugar reinforcement signaling pathway for classical olfactory conditioning in *Drosophila* larvae.

INDEXING TERMS: *Drosophila* larvae; neuropeptide F; single cell; learning and memory; reward; inhibition; BDSC_26263; BDSC_9681; BDSC_25681; BDSC_5137

http://doc.rero.ch

The mammalian neuropeptide Y (NPY) has received great attention because of its roles in regulating diverse aspects of behavior and physiology, including energy homeostasis, circadian rhythms, stimulation of food intake, reproduction, anxiety, seizure, alcohol addiction, learning, and memory (Kalra and Crowley, 1992; Zimanyi et al., 1998; Beck, 2001; Williams et al., 2001; Dyzma et al., 2010; Rotzinger et al., 2010). Invertebrate orthologs of the NPY family have been found in all major phyla (Nassel and Wegener, 2011). They are termed neuropeptide F (NPF) as the C-terminal tyrosine of vertebrates is exchanged to phenylalanine in invertebrates (Brown et al., 1999). In general, vertebrate NPY and invertebrate NPF exhibit an astonishing structural and functional conservation. For instance, a *Drosophila* NPY receptor homolog was shown to crossreact with human NPY family neuropeptides (Li et al., 1992). Thus, several of the behavioral and physiological NPY functions found in vertebrates were recently addressed in different invertebrate model systems (Wu et al., 2003, 2005d; Wen et al., 2005; Gonzalez and Orchard, 2008; Krashes et al., 2009; Hamasaka et al., 2010; Shohat-Ophir et al., 2012; Van Wielendaele et al., 2013)

The most extensive studies of NPF functions in invertebrates have been made in adult and larval *Drosophila*. Regulatory roles for *Drosophila* NPF (dNPF) are described for several behaviors including foraging, feeding, motivated feeding, ethanol sensitivity, nociception, aggression, reproduction, clock function, and learning

Grant sponsor: DFG; Grant numbers: TH1584/1-1 and TH1584/3-1; Grant sponsor: SNF; Grant number: 31003A_132812/1; Grant sponsor: Baden-Württemberg Stiftung and the Zukunftskolleg of the University of Konstanz (all to A.S.T.).

*CORRESPONDENCE TO: Andreas S. Thum, Department of Biology, University of Konstanz, Universitätsstraβe 10, 78464 Konstanz, Germany. E-mail: andreas.thum@uni-konstanz.de

(Shen and Cai, 2001; Wen et al., 2005; Wu et al., 2005d; Lee et al., 2006; Dierick and Greenspan, 2007; Xu et al., 2008, 2010; Krashes et al., 2009; Shohat-Ophir et al., 2012; Wang et al., 2013). The role of dNPF neurons in appetitive olfactory conditioning in larvae of *Drosophila*, however, was not analyzed. Yet several findings may suggest an involvement of dNPF neurons in appetitive olfactory conditioning in larvae. First, larvae exposed to fructose, which is usually used as the rewarding stimulus when analyzing appetitive olfactory learning, displayed a dose-dependent increase of dNPF-transcript in dNPF neurons located in the subesophageal ganglion (sog) (Shen and Cai, 2001). The sog region of the larval brain receives input from gustatory receptor neurons (GRN) of the peripheral nervous system (Colomb et al., 2007; Kwon et al., 2011). Output of GRN was shown to be important for appetitive and aversive gustatory-driven behaviors including choice behavior and feeding (Mishra et al., 2013; Apostolopoulou et al., 2014) and may potentially also contribute to the sugar reward signal. Second, dNPF signaling modulates motivated and gustatory-driven feeding. Larvae are constantly feeding but shortly before puparium formation they leave the food. This switch between feeding and wandering stage is regulated by dNPF since an overexpression extends the larval feeding phase and delays pupation (Wu et al., 2003). In addition, overexpression of the dNPF receptor (NPFR1) increases the intake of nonpalatable food (e.g., more solid food, bitter quinine containing food) (Wu et al., 2005a,d). Taken together, these results indicate that the dNPF signaling system is developmentally programmed to modify the dynamic regulation of gustatory driven food intake of different qualities. Such taste-dependent modulatory mechanisms might also affect appetitive olfactory learning. Third, fed larvae show increased feeding of sugar-rich food after a brief presentation of an appetitive food odor (Wang et al., 2013). The olfactory-driven change in behavior is absent when inhibiting the neuronal output of dNPF neurons or inactivating dNPF receptor function (Wang et al., 2013). Thus, these results suggest that the dNPF circuit modulates the rewarding function of certain food odors. Fourth, in adult *Drosophila* two studies showed that dNPF signaling is involved in appetitive olfactory learning by either modulating the retrieval of an appetitive olfactory memory based on the hunger state of the fly (Krashes et al., 2009), or by abolishing the conditioned preference for ethanol by changing the reinforcing function during training (Shohat-Ophir et al., 2012). Thus, in adult *Drosophila* dNPF neurons are involved in appetitive olfactory learning.

Drosophila larvae are able to form appetitive olfactory memories following odorant sugar reward pairing and a standardized behavioral paradigm exists for its analysis (Scherer et al., 2003; Neuser et al., 2005; Gerber and Stocker, 2007; Schipanski et al., 2008; Rohwedder et al., 2012; Apostolopoulou et al., 2013). Similar to other insects, it was shown that after appetitive olfactory conditioning a memory trace is established in Kenyon cells of the mushroom body (MB), a second-order "cortical" brain region (Honjo and Furukubo-Tokunaga, 2005; Pauls et al., 2010; Tomer et al., 2010; Michels et al., 2011). These results suggest a conserved function for the MB among developmental stages and different insect species with respect to olfactory learning (Heisenberg, 2003; McGuire et al., 2005; Keene and Waddell, 2007; Menzel, 2012; Farris, 2013). Larval MB Kenyon cells receive input from a small number of individually described olfactory projection neurons—second-order olfactory neurons (Masuda-Nakagawa et al., 2009, 2010; Thum et al., 2011). Projection neurons (PNs) in turn get direct sensory input from receptor neurons (ORNs: first-order olfactory neurons) that are assembled in the peripheral dorsal organ, the unique larval olfactory organ (Singh and Singh, 1984; Oppliger et al., 2000; Python and Stocker, 2002; Fishilevich et al., 2005; Kreher et al., 2005). Thus, a comprehensive functional description of the larval olfactory pathway exists almost on a single-cell level.

In contrast to olfactory processing, the neuronal pathways that signal sugar reward during classical olfactory conditioning in *Drosophila* larvae are largely unknown. There are no data available on the sensory neurons that collect and attribute the reward function to a presented sugar stimulus. This is still true, although anatomical and functional data is available for about 90 gustatory sensory neurons that are mainly involved in bitter and sugar taste-dependent choice behavior and feeding (Colomb et al., 2007; Kwon et al., 2011; Mishra et al., 2013; Apostolopoulou et al., 2014). Consequently, information on second-order neurons of the sugar reinforcement pathway is also not available.

However, there is evidence that the catecholamines, dopamine (DA), and octopamine/tyramine (OA/TA; tyramine being the precursor of OA) are specifically involved in sugar reward signaling in adult *Drosophila* (Schwaerzel et al., 2003; Kim et al., 2007, 2013; Burke et al., 2012; Liu et al., 2012; Lin et al., 2014; Huetteroth et al., 2015; Yamagata et al., 2015). Even more, several results allow for a similar assumption in larvae. First, activation of OA/TA neurons is sufficient to substitute for the reward during appetitive olfactory conditioning (Schroll et al., 2006). Second, OA/TA neurons or neuronal output of OA/TA neurons is necessary for signaling specific aspects of sugar reinforcement (e.g., nutritional value and sweetness) (Honjo and Furukubo-

http://doc.rero.ch

Tokunaga, 2009; Selcho et al., 2014). Third, neuronal output of DA neurons is necessary for appetitive olfactory conditioning (Selcho et al., 2009). However, in these experiments the innate gustatory-driven choice behavior towards fructose of the experimental animals is absent and thus a clear interpretation of the data is limited (Selcho et al., 2009). Fourth, mutant larvae lacking the dopamine receptor dDA1 are impaired in appetitive olfactory conditioning (Selcho et al., 2009). Together, these data suggest to some extent a conserved organization of reward processing in adult and larval *Drosophila* and additionally provide entry points for the identification of additional neuronal partners of the sugar reinforcement pathway.

Here we show results that extend the larval sugar reinforcement circuit required for appetitive olfactory conditioning by three pairs of dNPF neurons. In detail, we describe the larval dNPF neurons anatomically on the single-cell level including their input/output organization. We show that dNPF neurons and dNPF receptor function are necessary for appetitive olfactory learning using low sugar concentrations. This is not the case for high sugar concentrations. Furthermore, by using optogenetic and thermogenetic approaches we demonstrate that dNPF signaling specifically modulates the sugar-dependent reward information (unconditioned stimulus) during the training phase of the learning experiment.

MATERIALS AND METHODS

Fly strains

Flies were cultured according to standard methods (Selcho et al., 2009, 2014). For the behavioral experiments, UAS-*hid,rpr* (kindly provided by Simon Sprecher, University of Fribourg, Switzerland) (White et al., 1994, 1996; White and Steller, 1995; Kurada and White, 1998), UAS-*TRPA1* (Bloomington Fly Stock, Bloomington, IN, 26263; RRID:BDSC_26263) (Hamada et al., 2008), or UAS-*ChR2* (Bloomington Stock 9681; RRID:BDSC_9681) (Schroll et al., 2006) effector lines were crossed with the dNPF-Gal4 (kindly provided by Ping Shen, University of Georgia, Atlanta, GA; RRID:BDSC_25681) (Shen and Cai, 2001) driver line. Heterozygous controls were obtained by crossing Gal4-driver and UAS-effector with w^{1118} (kindly provided by Martin Heisenberg, University of Würzburg, Germany). In addition, we used the dNPF receptor mutant NPFR1 (Krashes et al., 2009) and an appropriate control of the same genetic background (kindly provided by Scott Waddell, University of Oxford, UK).

For visualizing neurons, we used the UAS-*mCD8::GFP* (Bloomington Stock 5137; RRID:BDSC_5137) (Lee and Luo, 1999). For creating single-cell flp-out clones, *y,w,hsp70-flp; Sp/CyO; UAS>CD2>mCD8::GFP/TM6b* virgins (kindly provided by Gary Struhl, Columbia University, New York, NY) (Wong et al., 2002) were crossed with dNPF-Gal4 males. A single heat shock was applied by placing vials containing eggs or larvae in a water bath at 37°C for 18 minutes. For the onset of heat shock, we chose different times from 0 to 200 hours after egg laying.

For analyzing the pre- and postsynaptic organization of the dNPF neurons we expressed UAS-*DenMark* (postsynaptic marker) and UAS-*syt::GFP* (presynaptic marker) via dNPF-Gal4 (RRID:BDSC_33064) (Nicolai et al., 2010).

For analyzing the behavior relevance of individual dNPF neurons we crossed *w+;UAS-stop-myc::TRPA1;pBPhsFLP2/TM6* flies (kindly provided by Barry Dickson, HHMI Janelia Farm Research Campus, USA) with dNPF-Gal4 (von Philipsborn et al., 2011).

Immunofluorescence

Immunostaining

Third instar larvae were put on ice and dissected in phosphate-buffered saline (PBS) (Selcho et al., 2009, 2012). Brains were fixed in 3.6% or 4% formaldehyde (Merck, Darmstadt, Germany) in PBS for 30 or 40 minutes. After rinsing in PBT (PBS with 3% or 0.3% Triton-X 100, Sigma-Aldrich, St. Louis, MO), brains were blocked with 5% normal goat serum (Vector Laboratories, Burlingame, CA) in PBT for 2 or 1.5 hours and then incubated for up to 2 days with primary antibodies at 4°C. Before applying the secondary antibodies for up to 2 days at 4°C, brains were washed with PBT. Finally, brains were washed with PBT and mounted in Vectashield (Vector Laboratories) or 80% glycerol (Sigma-Aldrich) between two coverslips and stored at 4°C in darkness.

Antibodies

To visualize the total expression pattern of dNPF-Gal4 and the innervation patterns of single dNPF-Gal4-positive neurons, we applied a polyclonal serum against green fluorescent protein (anti-green fluorescent protein [GFP], A6455; Molecular Probes, Eugene, OR; 1:1,000; RRID: AB_221570; Table 1) in combination with two different mouse antibodies labeling the neuropil (anti-ChAT, ChAT4B1, anti-choline acetyltransferase; DSHB, Iowa City, IA; 1:100; RRID: AB_528122; Table 1) and axonal tracts (anti-FasII, 1d4, antifasciclin II; DSHB; 1:55; RRID: AB_528235; Table 1), respectively. To label the pre- and postsynaptic structures of the dNPF1-Gal4-positive neurons we used a conjugated goat GFP FITC antibody (ab 6662, Abcam, Cambridge, MA, 1:1000; RRID: AB_305635; Table 1) that binds to *syt::GFP*. In

http://doc.rero.ch

TABLE 1.
Primary Antibodies

Antibody	Host	Immunogen	Manufacturer	Working dilution	RRID
Anti-GFP	Rabbit, polyclonal serum	Purified green fluorescent protein (GFP), a 27-kDa protein derived from the jellyfish Aequorea victoria	A6455, Molecular Probes (Eugene, OR, USA)	1:1000	AB_221570
Anti-GFP-FITC conjugated	Goat, polyclonal to GFP	Recombinant full length protein corresponding to GFP aa 1-246	ab6662, abcam (Cambridge, UK)	1:1000	AB_305635
Anti-GFP	Mouse, monoclonal	Purified green fluorescent protein (GFP) derived from the jellyfish *Aequorea Victoria*	A11120, Moleculare Probes (Eugene, OR, USA)	1:200	AB_221568
ChAT4B1	Mouse, monoclonal	80-kDa Drosophila choline acetyltransferase protein	ChAT4B1, DSHB (Iowa City, IA, USA)	1:100	AB_528122
1D4 anti-Fasciclin II	Mouse, monoclonal	Bacterially expressed fusion peptide containing the intracellular C-terminal 103 amino acids of the PEST transmembrane form of FasII	1D4, DSHB (Iowa City, IA, USA)	1:55	AB_528235
Anti-DsRed	Rabbit, polyclonal serum	DsRed-Express, a variant of Discosoma red fluorescent protein	632496, Clonetech (Mountain View, CA, USA)	1:200	AB_10013483
Anti-TH	Rabbit, polyclonal serum	A PCR-generated 1.5 kb fragment with Nde I linkers containing only the DTH coding region	gift from W. Neckameyer	1:800	
Anti-dNPF	Rabbit, polyclonal serum	The antiserum was raised against a 36-residue, COOH-terminus amidated synthetic peptide corresponding to a deduced mature dNPF (SLMDILRNHEMDNINLGKN ANNGGEFARGFNEEEIF)	gift from P. Shen (University of Georgia, GA, USA)	1:1000	AB_2314965
Anti-myc	Mouse, monoclonal	epitope (EQKLISEEDL) derives from a protein sequence in the human protooncogene p62 c-myc	9E10; DSHB (Iowa City, IA, USA)	1:50	AB_2266850
Anti-TDC	Rabbit, polyclonal serum	synthetic peptides derived from C-terminal part of Drosophila melanogaster Tdc2 protein: NH2-CFNSNN-EEKGSNVCO-NH2 and NH2-CAVRKA-SSTRDNLNCO-OH	pab0822-P, Covalab (St John's Innovation Centre, Cambridge, UK)	1:200	

http://doc.rero.ch

addition, rabbit anti-DsRed (632496, Clonetech, Palo Alto, CA, 1:200; RRID: AB_10013483, Table 1) was used to visualize the postsynaptic structures by recognizing DenMark (Nicolai et al., 2010). The neuropil was also stained by anti-ChAT (ChAT4B1, anticholineacetyltransferase; DSHB, 1:100; RRID: AB_528122; Table 1) and anti-FasII (1d4, antifasciclin II; DSHB; 1:55; RRID: AB_528235; Table 1). To identify single neurons in the TRPA flp out experiment mouse anti-myc (9E10; DSHB, 1:50; RRID: AB_2266850; Table 1) was applied (von Philipsborn et al., 2011). To confirm the ablation of dNPF neurons with UAS-*hid,rpr*, crosses of dNPF-Gal4/UAS-*hid,rpr* and heterozygous control animals were analyzed using an anti-dNPF antibody preincubated with C8 peptide (gift from P. Shen; University of Georgia, 1:1,000; RRID: AB_2314965; Table 1). Overlay of dNPF and DA neurons was investigated using a double-staining of rabbit anti-TH (kind gift of Wendi Neckameyer, 1:800; Table 1) and a monoclonal mouse anti-GFP antibody (A11120, mAB 3E6, Molecular Probes, Carlsbad, CA, 1:200; RRID: AB_221568; Table 1). Overlay of dNPF and OA/TA (Pech et al., 2013) neurons was investigated using a double-staining of rabbit anti-TDC (pab0822-P, Covalab, 1:200; Table 1) and a monoclonal mouse anti-GFP antibody (A11120, mAB 3E6, Molecular Probes, 1:200; RRID: AB_221568; Table 1).

As secondary antibodies, goat antirabbit IgG Alexa Fluor 488 (A11008; Molecular Probes; 1:200; RRID: AB_143165), goat antimouse IgG Alexa Fluor 647 (A21235, Molecular Probes, 1:200; RRID: AB_10374721),

goat antimouse IgG Cy3 (A10521, Molecular Probes, 1:200; RRID: AB_10373848), goat antirabbit IgG Cy5 (A10523, Molecular Probes, 1:200; RRID: AB_10374302), goat antimouse DyLight488 (Jackson ImmunoResearch, Dianova, Göttingen, Germany, 1:200) and goat antirabbit DyLight649 (Jackson ImmunoResearch, 1:200) were used.

Antibody characterization

Anti-GFP

The rabbit anti-GFP antibody gave the same staining pattern in the central nervous system (CNS) of the dNPF-Gal4/UAS-*mCD8::GFP* larvae as the conjugated goat anti-GFP FITC antibody and the mouse anti-GFP antibody. Additionally, staining was not observed in the CNS of larvae expressing only dNPF-Gal4 or only UAS-*mCD8::GFP* (data not shown).

Anti-GFP-FITC conjugated

The conjugate goat anti-GFP-FITC antibody recognizes in immunoelectrophoresis assays a single precipitin arc against anti-goat serum anti-fluorescein and purified and partially purified green fluorescent protein (*Aequorea victoria*). In our experiments the antibody gave the same staining pattern in the CNS of the dNPF-Gal4/UAS-*mCD8::GFP* larvae as the rabbit anti-GFP antibody.

Anti-GFP

The mouse anti-GFP antibody gave the same staining pattern in the CNS of the dNPF-Gal4/UAS-*mCD8::GFP* larvae as the rabbit anti-GFP and conjugated goat anti-GFP FITC antibodies. Additionally, staining was not observed in the CNS of larvae expressing only dNPF-Gal4 or only UAS-*mCD8::GFP* (data not shown).

ChAT4B1

The anti-ChAT antibody was shown to label a single band at a position of about 80 kDa in crude fly head samples (Takagawa and Salvaterra, 1996).

1D4 anti-Fasciclin II

The anti-FasII antibody labeled a 97-kDa band in western blot, which was gone in FasII null mutants (Grenningloh et al., 1991; Mathew et al., 2003). The staining pattern observed in this study is identical to previous reports (Grenningloh et al., 1991; Mathew et al., 2003).

Anti-DsRed

Anti-DsRed targets Discosoma red fluorescent protein (RFP). The fusion gene DenMark (a hybrid protein of the mouse protein ICAM5/telencephalin and the red fluorescent protein mCherry) (Nicolai et al., 2010) was reported to be recognized by anti-DsRed in neurons of the CNS of adult *Drosophila* (Bidaye et al., 2014). Antibody enhancement of the DenMark signal in our experiments is consistent with the known expression pattern of dNPF-Gal4 (Shen and Cai, 2001).

Anti-TH

A polyclonal antibody against *Drosophila* tyrosine hydroxylase (DTH) was raised in rabbits using bacterially expressed protein as antigen (Neckameyer et al., 2000). A polymerase chain reaction (PCR)-generated 1.5 kb fragment with Nde I linkers containing only the DTH coding region was subcloned into the Nde I site of the *Escherichia coli* expression vector pET11a and transformed in BL21/DE3 cells. The anti-TH serum was used in *Drosophila* larvae before (Selcho et al., 2009); the expression pattern in the CNS strongly correlates with the expression of TH-Gal4; UAS-*mCD8::GFP* when analyzed on the single-cell level.

Anti-dNPF

The rabbit antiserum was raised against a 36-residue, COOH-terminus amidated synthetic peptide corresponding to a deduced mature dNPF (Shen and Cai, 2001). To ensure its specificity, the antiserum was preabsorbed against a synthetic amidated octapeptide (C8) corresponding to the carboxyl structure of dNPF, which is conserved among a number of different neuropeptides. It was reported that the preabsorbed anti-dNPF expression pattern matches whole mount in situ RNA hybridization experiments for dNPF within the larval CNS (Shen and Cai, 2001).

9E10 anti-myc

The 9E10 antibody epitope (EQKLISEEDL) derives from a protein sequence in the human protooncogene p62 c-myc and is widely used as a protein fusion tag (Hilpert et al., 2001).

Anti-TDC

The rabbit polyclonal antiserum was raised against synthetic peptides derived from C-terminal part of *Drosophila melanogaster* Tdc2 protein: NH2-CFNSNN-EEKGSNVCO-NH2 and NH2-CAVRKA-SSTRDNLNCO-OH. The antiserum was used in adult and larval *Drosophila*. Ablation of OA/TA neurons in the larval brain correlated with the absence of a specific staining for OA and TA neurons (Pech et al., 2013; Pauls et al., 2015).

Microscopy and figure production

CNS preparations were scanned using a confocal light scanning microscope (LeicaTCS SP5; Leica TCS SP8; Leica Microsystems, Wetzlar, Germany, and Zeiss LSM510M; Carl Zeiss Microscopy; Göttingen, Germany). The images scanned with a step size of 1 μm or 0.8 μm thicknesses

http://doc.rero.ch

were analyzed in the software program ImageJ (NIH, Bethesda, MD). Contrast, brightness, and coloring were adjusted in Photoshop (Adobe Systems, San Jose, CA).

Behavioral experiments

Odor-fructose learning

Appetitive olfactory learning was tested by using standardized, previously described assays (Scherer et al., 2003; Neuser et al., 2005; Schipanski et al., 2008; Pauls et al., 2010; Rohwedder et al., 2012; Apostolopoulou et al., 2013). In detail, all learning experiments were conducted on assay plates filled with a thin layer of agarose solution containing either pure 2.5% agarose or 2.5% agarose plus fructose at concentrations of 2M or 0.02M. As olfactory stimuli, we used 10 µl amyl acetate (AM Fluka, Buchs, Switzerland, Cat. No. 46022; diluted 1:250 in paraffin oil, Fluka Cat. No. 76235) and 10 µl benzaldehyde (BA, undiluted, Fluka Cat. No. 12010). Odorants were loaded into custom-made Teflon containers (4.5-mm diameter) with perforated lids as described by Scherer et al. (2003). Learning ability was tested by exposing a first group of 30 animals to BA while crawling on agarose medium containing sugar as a positive reinforcer. After 5 minutes, larvae were transferred to a fresh Petri dish in which they were allowed to crawl on pure agarose medium for 5 minutes while being exposed to AM. The training was repeated three times if not otherwise stated. A second group of larvae received reciprocal training. Immediately after training larvae were transferred onto test plates on which AM and BA were presented on opposite sides. After 5 minutes, individuals were counted on the AM side (No. AM), the BA side (No. BA), and in a 1-cm neutral zone in between (for further details a video is available in Apostolopoulou et al., 2013). Due to the stressful heat and the light treatment applied in experiments for artificial thermal and light activation of dNPF neurons we reduced the training intervals to 2.5 minutes per plate in these experiments. By subtracting the number of larvae on the BA side from the number of larvae on the AM side divided by the total number of counted individuals (No. total), we calculated a preference index for each training group:

$$\mathrm{PREF}_{\mathrm{AM+/BA}} = (\mathrm{No.\,AM} - \mathrm{No.\,BA} \,/\, \mathrm{No.\,total})$$
$$\mathrm{PREF}_{\mathrm{AM/BA+}} = (\mathrm{No.\,AM} - \mathrm{No.\,BA} \,/\, \mathrm{No.\,total})$$

We then compiled a performance index (PI):

$$\mathrm{PI} = (\mathrm{PREF}_{\mathrm{AM+/BA}} - \mathrm{PREF}_{\mathrm{AM/BA+}}) \,/\, 2$$

Negative PIs represent aversive learning, whereas positive PIs indicate appetitive learning.

Odor-salt learning

Odor-salt learning was performed as described above for appetitive olfactory learning (Gerber and Hendel, 2006; Schleyer et al., 2011). However, fructose as reinforcer was replaced by 1.5M sodium chloride (VWR International, AnalaR Normapur, Cat. No. 27810.295). Sodium chloride was added to one of the training plates and to the test plate. Preference and performance indices were calculated accordingly.

Heat activation

To artificially activate dNPF neurons using UAS-*TRPA1* (Hamada et al., 2008; Krashes et al., 2009), cohorts of 30 larvae were placed into vials filled with a layer of 2.5% agarose to prevent dehydration. For all heat activation experiments, vials with larvae were then set into a water bath (36°C) for 5 minutes for preincubation; directly afterwards learning experiments, feeding experiments, and acuity tests were performed at 32–34°C in a custom-made heat chamber.

Light activation

For light activation, larvae were raised at 25°C in the dark on standard corn medium, to which 2.5 mM all-trans-retinal (Sigma-Aldrich, Cat. No. R2500) diluted in ethanol was added (Schroll et al., 2006). The plates for training and test were placed above a set of four high-power LEDs (Luxeon I Star LED, Luxeon) emitting blue light (∼465 nm) at ∼20 000 Lux. In the activation during training, 30 feeding third instar larvae were placed onto the training plates, which were then covered by a mirrored box. The learning paradigm was performed as described above. Light was turned on and off in 30-second intervals during the cycles. The test was performed in the dark. For activating during test the larvae were trained in the dark and exposed to light during the test phase. Again, light was turned on and off in 30-second intervals. In contrast to heat activation there was no preincubation phase with blue light in these experiments.

Substitution experiment

To substitute the presentation of a sugar reward by artificially activating neurons we used UAS-*ChR2*;UAS-*ChR2* (Schroll et al., 2006). Thirty feeding third instar larvae were placed onto plates containing 2.5% agarose and exposed to either BA or AM. During the presentation of the first odor the larvae were exposed to blue light (∼465 nm, ∼20,000 Lux) for 5 minutes. The second odor was then presented in the dark. As described for appetitive olfactory learning, the training was performed by training two groups reciprocally. The sequence of light/dark presentation was randomized. Performance indices were calculated as described above.

http://doc.rero.ch

Single cell activation

To investigate single neurons of the dNPF circuit in olfactory associative learning we crossed *w*$^{+}$*;*UAS-*stop-myc::TRPA1;pBPhsFLP2/TM6* to dNPF1-Gal4 to then use a protocol that was developed for flies (von Philipsborn et al., 2011). In detail, we applied a heat shock (36°C) 48–72 hours after egg laying. The heat-shock was reduced to 6 minutes to flip only no cells or single cells within a larval brain. Cohorts of 30 feeding third instar larvae were then trained as described in "Heat activation" (above). After testing, larvae were separated into groups that preferred the rewarded odor and groups that did not. The larvae were directly dissected and the brains stained with anti-myc (9E10; DSHB, 1:50) using the described standard immunohistochemistry protocol to identify every cell that expressed myc::TRPA1 in each larval brain. Finally, learners and no-learners were separated for each cell type and a mean value was calculated for each cell type by counting learners as 1 and nonlearners as –1.

Gustatory preference

For gustatory preference tests, 2.5% agarose solution (Sigma-Aldrich) was boiled in a microwave oven and filled as a thin layer into Petri dishes (85 mm diameter; Sarstedt) (Apostolopoulou et al., 2013). After cooling, the agarose was removed from half of the plate. The empty half was filled with 2.5% agarose solution containing fructose (0.02M or 2M). Assay plates were used on the same day. Groups of 30 larvae were placed in the middle of the plate, allowed to crawl for 5 minutes, and then counted on the sugar side, the sugar-free agarose side, and a 1-cm wide neutral zone in between. By subtracting the number of larvae on the pure agarose side (No. nS) from the number of larvae on the sugar side (No. S) divided by the total number of counted larvae (No. total), a Preference Index was calculated:

$$\mathrm{PREF} = (\mathrm{No.\,S} - \mathrm{No.\,nS}) \,/\, \mathrm{No.\,total})$$

Negative PREF values indicate sugar avoidance, whereas positive PREF values represent sugar attractiveness. The values given in Table 2 are mean values and SEM. The sample size is 15 for each group in each experiment. Light and heat activation protocols were applied as described above.

Olfactory preference

For olfactory acuity test, 2.5% agarose solution (Sigma-Aldrich) was boiled in a microwave oven and filled as a thin layer into Petri dishes (85 mm diameter, Sarstedt) (Apostolopoulou et al., 2013). After cooling, closed Petri dishes were kept at room temperature and were used on the same day. Then, 10 µl of either pure benzaldehyde or diluted amylacetate (1:250 in paraffin oil) were loaded into a Teflon container (Apostolopoulou et al., 2013). Olfactory preferences were tested by placing 30 larvae in the middle of the Petri dish with an odor-containing Teflon container on one side and an empty container on the other side.

The position of each larva was counted on the odor side, the odor-free side, and a 1-cm wide neutral zone in between. By subtracting the number of larvae on the odor-free side (No. nO) from the number of larvae on the odor side (No. O) divided by the total number of counted larvae (No. total), a Preference Index was calculated:

$$\mathrm{PREF} = (\mathrm{No.\,O} - \mathrm{No.\,nO}) \,/\, \mathrm{No.\,total})$$

Negative PREF values indicate odor avoidance, whereas positive PREF values represent odor attractiveness. The values given in Table 2 are mean values and SEM. The sample size is 15 for each group in each experiment. Light and heat activation protocols were applied as described above.

Starvation

For starvation experiments, cohorts of 30 larvae were collected and rinsed with tap water to remove remaining food. The larvae were then put onto Petri dishes filled with 2.5% agarose and covered with a thin layer of water to prevent dehydration. The Petri dishes were closed with a lid to keep the larvae from escaping the dish. After 60 or 180 minutes, respectively, larvae were then transferred to the experimental plates.

Feeding

To measure feeding behavior, 30 feeding third instar larvae were placed on a Petri dish containing fructose at a concentration of 2M, dissolved in 1% agarose and 2% indigocarmin (Sigma-Aldrich, Cat. No. 73436). An additional control group was put on pure agarose plates containing only 1% agarose and 2% indigocarmin. Larvae from all these groups were allowed to feed on this substrate for 30 minutes, washed in tap water, and, as a group, homogenized in 500 µl of a 1M ascorbic acid solution (Sigma-Aldrich, Cat. No. A7506). The homogenate was centrifuged for 5 minutes at 13,400 rpm. The supernatant was then filtered using a syringe filter (millipore, 5-µm pores) into a fresh Eppendorf cup and centrifuged again for 5 minutes at 13,400 rpm. In all, 100 µl of the supernatant was loaded into single wells of a 96-well plate (Hartenstein, Würzburg, Germany). Then, using an Epoch spectrophotometer (BioTek, Bad Friedrichshall, Germany), absorbance at 610 nm was measured. The results are presented as absorbance of

http://doc.rero.ch

http://doc.rero.ch

TABLE 2.

Olfactory Acuity and Taste Perception

loss of NPF function experiments:

	UAS-hid,rpr	dNPF-Gal4	dNPF-Gal4 UAS-hid,rpr	Difference between groups	WT	NPFR1	Difference between groups
Odor preference							
Benzaladehyde	0.51 ± 0.05	0.21 ± 0.08	0.49 ± 0.04	n.s. except $p<0.05$ dNPF-Gal4 compared to UAS-hid,rpr and dNPF-Gal4; UAS-hid,rpr	0.44 ± 0.08	0.39 ± 0.06	n.s.
Amylacetat	0.10 ± 0.05	0.20 ± 0.07	0.39 ± 0.06	n.s. except $p<0.05$ UAS-hid,rpr compared to dNPF-Gal4; UAS-hid,rpr	0.30 ± 0.07	0.17 ± 0.06	n.s.
Sugar Preference							
0.02 M Fructose	0.28 ± 0.07	0.34 ± 0.06	0.43 ± 0.07	n.s.	0.17 ± 0.08	0.20 ± 0.07	n.s.
2M Fructose	n.d.	n.d.	n.d.		0.27 ± 0.06	0.17 ± 0.05	n.s.

gain of NPF function experiments:

	UAS-TRPA1	dNPF-Gal4	dNPF-Gal4 UAS-TRPA1	Difference between groups	UAS-ChR2	dNPF-Gal4	dNPF-Gal4 UAS-ChR2	Difference between groups
Odor preference								
Benzaladehyde	0.17 ± 0.06	0.15 ± 0.06	0.08 ± 0.06	n.s.	0.18 ± 0.05	0.22 ± 0.06	0.12 ± 0.06	n.s.
Amylacetat	0.15 ± 0.05	0.36 ± 0.05	0.28 ± 0.03	n.s.	0.26 ± 0.09	0.24 ± 0.07	0.22 ± 0.06	n.s.
Sugar Preference								
2M Fructose	0.50 ± 0.05	0.67 ± 0.04	0.39 ± 0.05	n.s. except $p<0.05$ dNPF-Gal4 compared to dNPF-Gal4; UAS-TRPA1	0.31 ± 0.06	0.21 ± 0.06	0.29 ± 0.03	n.s.
Learning experiments at permissive temperature								
	0.31 ± 0.06	0.30 ± 0.06	0.23 ± 0.03	n.s.				

Sample Size: n = 15.
values are given as mean and SEM.
n.s.: no significant difference.
for heat induction a preincubation of 5 minutes was applied; for light induction no preincubation was used.

the sample minus blank (Rohwedder et al., 2012). To activate the neurons during feeding the plates were prepared as described and placed into a custom-made heating box (32–34°C, 75% humidity) and the larvae allowed to feed for 30 minutes.

Statistical analysis

For all experiments that analyze behaviors of *Drosophila* larvae the data for all different groups were collected in parallel. To compare across multiple groups a Kruskal–Wallis test followed by Wilcoxon rank sum test and Holm–Bonferroni correction was performed. The Wilcoxon signed ranked test was used to compare one group against chance level. Statistical analysis was performed with R v. 2.14.0 and Windows Excel 2010. Figure alignments were adjusted in Adobe Photoshop. The data are presented as whisker-boxplots. The middle line within the box shows the median, the box boundaries refer to the 25 and 75% quantiles, and the whiskers represent the 10 and 90% quantiles. Small circles indicate outliers. Asterisks shown in the figures indicate significance levels: n.s. for $P > 0.05$, * for $P < 0.05$, ** for $P < 0.01$, and *** for $P < 0.001$.

RESULTS

Anatomy of the dNPF neurons on single-cell level

It was reported that the larval brain covers only six dNPF-positive neurons (Shen and Cai, 2001). To visualize the detailed anatomy of the dNPF neurons we expressed UAS-*mCD8::GFP* via dNPF-Gal4 and marked the neurons in whole-mount preparations via anti-GFP staining and neuropil structures by anti-choline acetyltransferase/anti-Fasciclin2 (ChAT/Fas2) staining (Fig. 1A–F) (Lee and Luo, 1999; Selcho et al., 2009). In line with earlier reports (Shen and Cai, 2001), we find that dNPF-Gal4 drives expression in three pairs of neurons that innervate the entire larval brain at defined regions (see later description for specific details, Fig. 1A–F). The soma of each of the three cell types are located very lateral in the hemispheres, slightly lateral in the hemispheres and in the sog, respectively (Fig. 1A,B). To untangle the input/output organization of these six neurons we expressed a presynaptic marker UAS-*synaptotagmin::GFP* and a postsynaptic marker UAS-*Denmark::mCherry* at the same time via dNPF-Gal4 (Fig. 2A–P) (Nicolai et al., 2010). Using an anti-GFP antibody (presynaptic), an anti-red fluorescent protein (RFP) antibody (postsynaptic), and an anti-ChAT/Fas2 antibody mixture (neuropil) at the same time we demonstrate that the dNPF neuron innervation in lateral regions of the hemispheres is dominantly postsynaptic (Fig. 2A–H). The dNPF neuron innervation in dorsomedial protocerebrum mainly gives rise to presynapses (Fig. 2E–H). The expression in the sog is both presynaptic and postsynaptic (Fig. 2I–L). The long descending projections from the hemispheres along the ventral nerve cord (vnc) are only presynaptic (Fig. 2M–P).

Although the expression pattern of dNPF-Gal4 is already very sparse, it was not possible to identify the morphology of each neuron distinctly in the complete pattern due to the wide and overlapping innervation of these neurons. Therefore, we applied the flp-out technique to mark each neuron individually (Wong et al., 2002). We prepared about 200 brain samples that individually labeled three clearly distinct cell types multiple times (Fig. 3). Based on the position of the cell body we called the cells: dNPF-DL1 (dorsolateral cell 1), dNPF-DL2 (dorsolateral cell 2), and dNPF-sog (subesophageal ganglion). dNPF-DL1 has its cell body situated posterior in the dorsolateral protocerebrum (dlp) (Fig. 3A–D). A huge branch innervates mainly the basolateral protocerebrum (blp) and to a smaller degree also the dlp. Here its innervation is mostly postsynaptic and splits several times (Fig. 3C). The presynaptic branch of the neuron crosses the midline and projects medially down through the contralateral sog to the vnc (Fig. 3B–D). At the end of the vnc the neuron loops back at least one abdominal segment (Fig. 3D). dNPF-DL2 has its cell body located anteriorly very lateral in the dorsal protocerebrum (dlp) (Fig. 3G). The neuron has several postsynaptic branches located ipsilaterally in the dlp (Fig. 3G). Presynaptic structures are visible in the ipsilateral dorsomedial protocerebrum (dmp) and on a more restricted level at the ipsilateral dlp and basomedial protocerebrum (bmp) (Fig. 3G,H). dNPF-sog shows the typical morphology of a gustatory interneuron as it has pre- and postsynaptic structures located only locally in the ipsi- and contralateral sog at a region that potentially overlaps with terminals of gustatory receptor neurons (Fig. 3I,J). Furthermore, a double clone of the dNPF-sog neurons of both hemispheres shows that their branches within the sog overlap (Fig. 3K). Taken together, we analyzed the detailed anatomy of the six dNPF neurons in the larval brain on the single-cell input/output structure level. This information is a necessary initial step to anatomically evaluate if dNPF neurons do connect with the sugar reinforcement pathway of the larval brain.

Based on this assumption we tested if dNPF neurons do colocalize with dopaminergic (DA) and tyraminergic and octopaminergic (TA/OA) neurons in the larval brain (Fig. 4) (Selcho et al., 2009, 2012, 2014). Third instar larval brains of the dNPF-Gal4 strain crossed with UAS-nsyb::GFP double-labeled by anti-GFP (to visualize dNPF

http://doc.rero.ch

http://doc.rero.ch

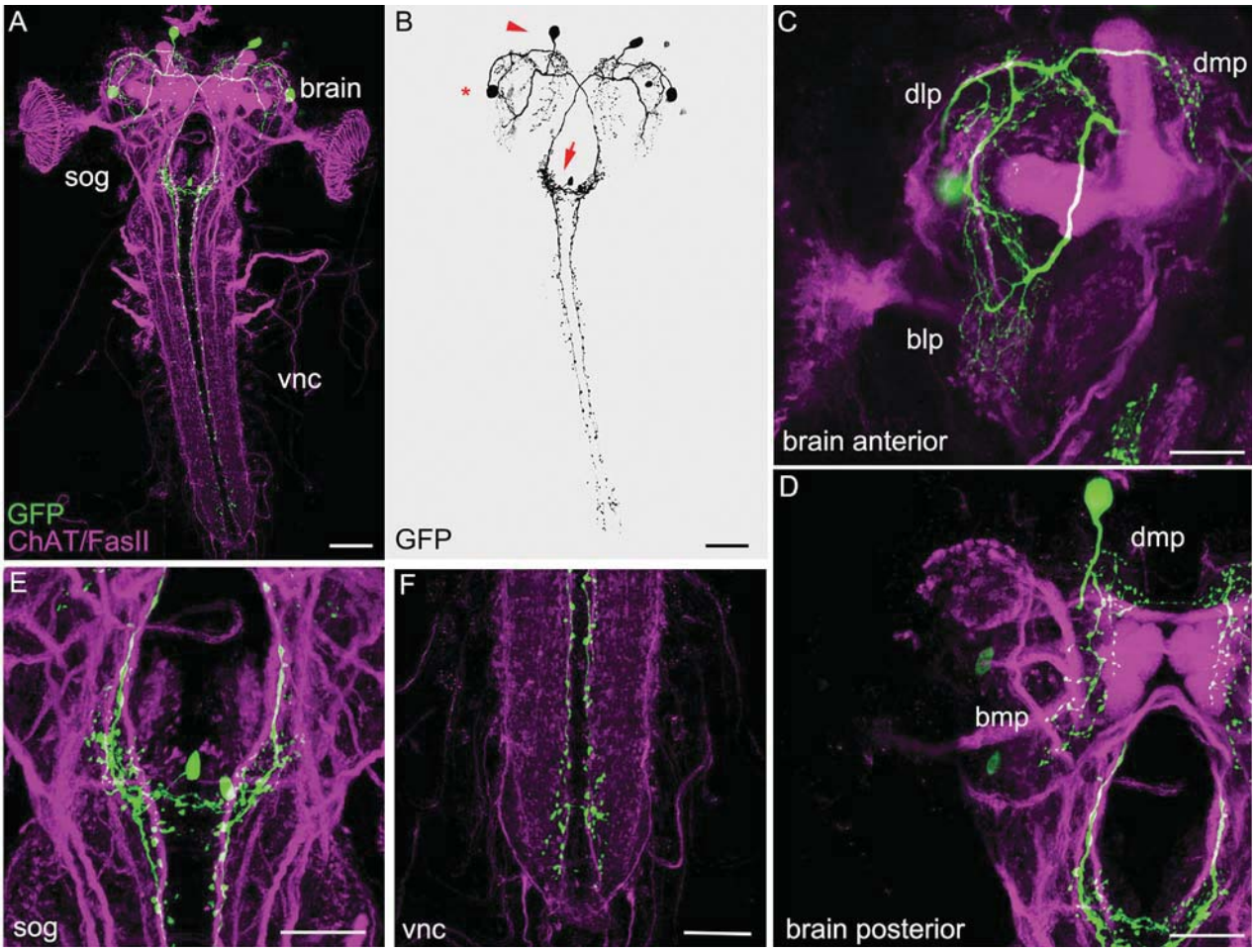

Figure 1. Anatomy of the dNPF neuronal circuit. **A:** Frontal view projection of a dNPF-Gal4/UAS-*mCD8::GFP* larval brain. Three pairs of GFP-positive neurons are visible (green) in the larval central nervous system (magenta) that innervate defined regions of the brain, subesophageal ganglion (sog), and ventral nerve cord (vnc); magenta: anti-choline actetyltransferase (ChAT) and anti-Fasciclin II (FasII); green: anti-GFP (GFP). **B:** Only the GFP channel is shown from A, which highlights the labeling of the three pairs of dNPF-Gal4-positive neurons. In the following the individual neurons are called dNPF-DL1 (arrowhead), dNPF-DL2 (asterisk), and dNPF-sog (arrow) based on their cell body position. **C–F:** Magnified views of partial projections for the anterior brain (C), posterior brain (D), sog (E), and vnc (F). The six dNPF-positive neurons innervate specific regions of the dorsolateral protocerebrum (dlp), basolateral protocerebrum (blp), dorsomedial protocerebrum (dmp), basomedial protocerebrum (bmp), the sog, and vnc. Scale bars = 50 μm in A,B; 25 μm in C–F.

neurons) and anti-TH (tyrosine hydroxylase, to visualize DA neurons) showed potential overlap of the two circuits in the dmp, at a lower level within the blp (Fig. 4D–F) and dlp (Fig. 4G–I). In contrast, anti-TDC staining of TA/OA neurons with dNPF-Gal4;UAS-*nyb::GFP* was very sparse in the larval brain hemispheres (Fig. 4J–R). Potential overlap was detectable in the dmp and dlp (Fig. 4P–R). Yet strong overlap was visible in the sog, the first integration center of gustatory information within the larval brain (Fig. 4M–O).

Hence, based on a purely anatomical argument, dNPF neurons may be able to modulate the DA and TA/OA reinforcing system of the larval brain. Nevertheless, we want to mention that dNPF acts as a neuropeptide over larger distances than the synaptic cleft (Nassel and Wegener, 2011). Thus, these results provide only limited information on the role of dNPF in appetitive olfactory conditioning and behavioral experiments have to further support this hypothesis.

dNPF signaling is necessary for olfactory learning using a low sugar concentration

Drosophila larvae are able to associate odors with fructose reward. This particular behavior can be parametrically analyzed since a standardized assay exists (Scherer et al., 2003; Neuser et al., 2005; Schipanski et al., 2008; Rohwedder et al., 2012; Apostolopoulou et al., 2013). In short, larvae are trained with two odors, one of which is presented together with the

http://doc.rero.ch

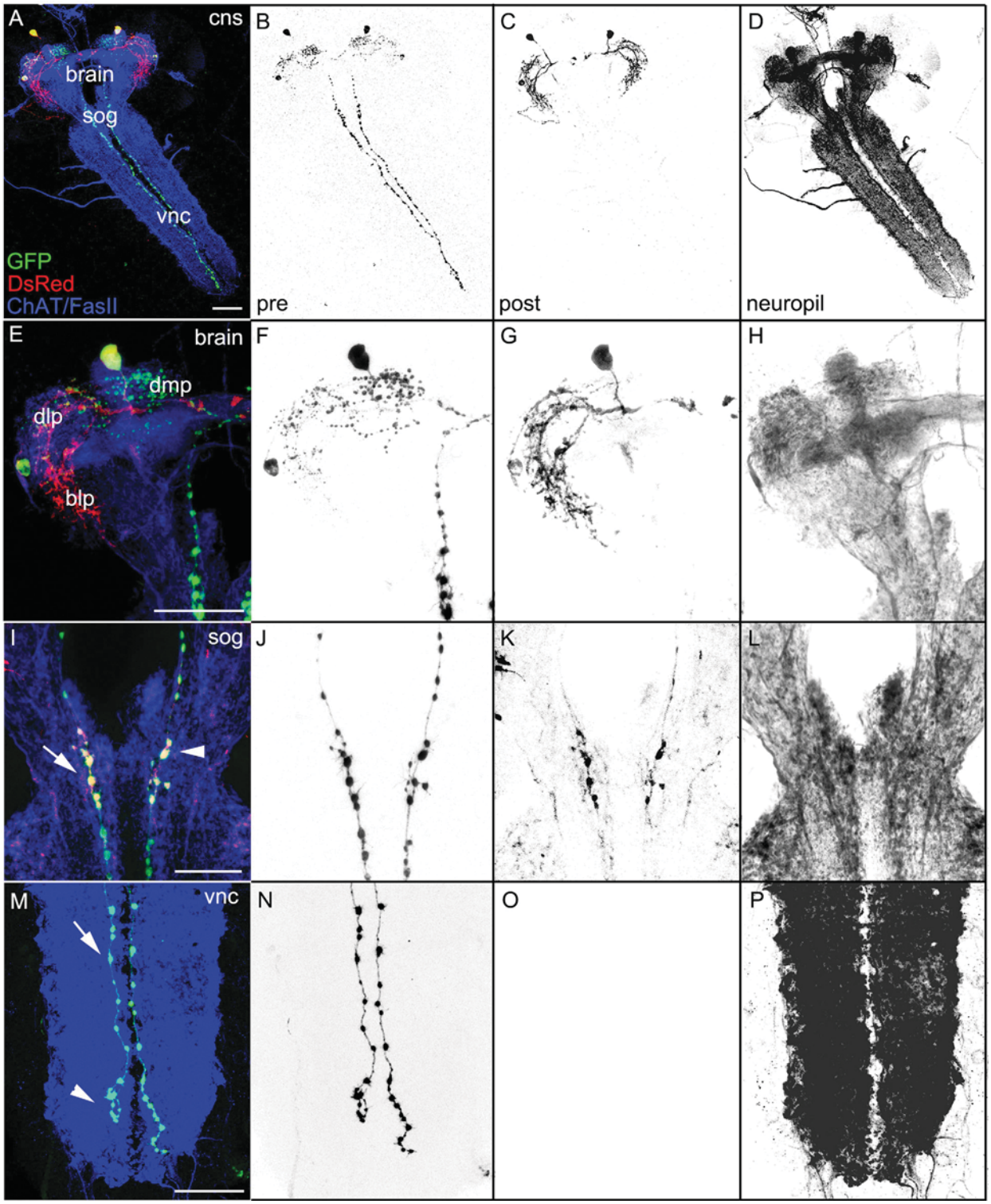

Figure 2. Pre- and postsynaptic organization of the dNPF neuronal circuit. The figure shows complete and partial frontal projections of the central nervous system of dNPF-Gal4; UAS-*DenMark,* UAS-*syt::GFP* larvae. UAS-*syt::GFP* (blue; anti-ChAT/anti FasII) labels presynaptic bouton-like structures (green; UAS-*syt::GFP*; GFP), whereas UAS-*DenMark* is reported to be expressed in postsynaptic regions of neurons (red; UAS-*DenMark*, DsRed). The entire CNS is shown in **A,** a single hemisphere is depicted in **E,** the sog and vnc are shown in **I,M,** respectively. **B,E,I,M:** UAS-*syt::GFP* staining in black. **C, G, K and O** UAS-*DenMark* in black. **D,H,L,P:** Neuropil staining in black. Postsynaptic staining was detectable in the blp, dlp, sog (arrow and arrowhead in I), and weakly in the dmp. In addition, the dlp, dmp, sog (arrow and arrowhead in I), and vnc (arrow and arrowhead in M)) are presynapticaly innervated by the dNPF neurons. Please also notice that dNPF-Gal4; UAS-*DenMark,* UAS-*syt::GFP* expression was weaker in the sog compared to dNPF-Gal4; UAS-*mCD8::GFP* expression (Fig. 1). Scale bars = 50 μm in A–D; 25 μm in E–P.

http://doc.rero.ch

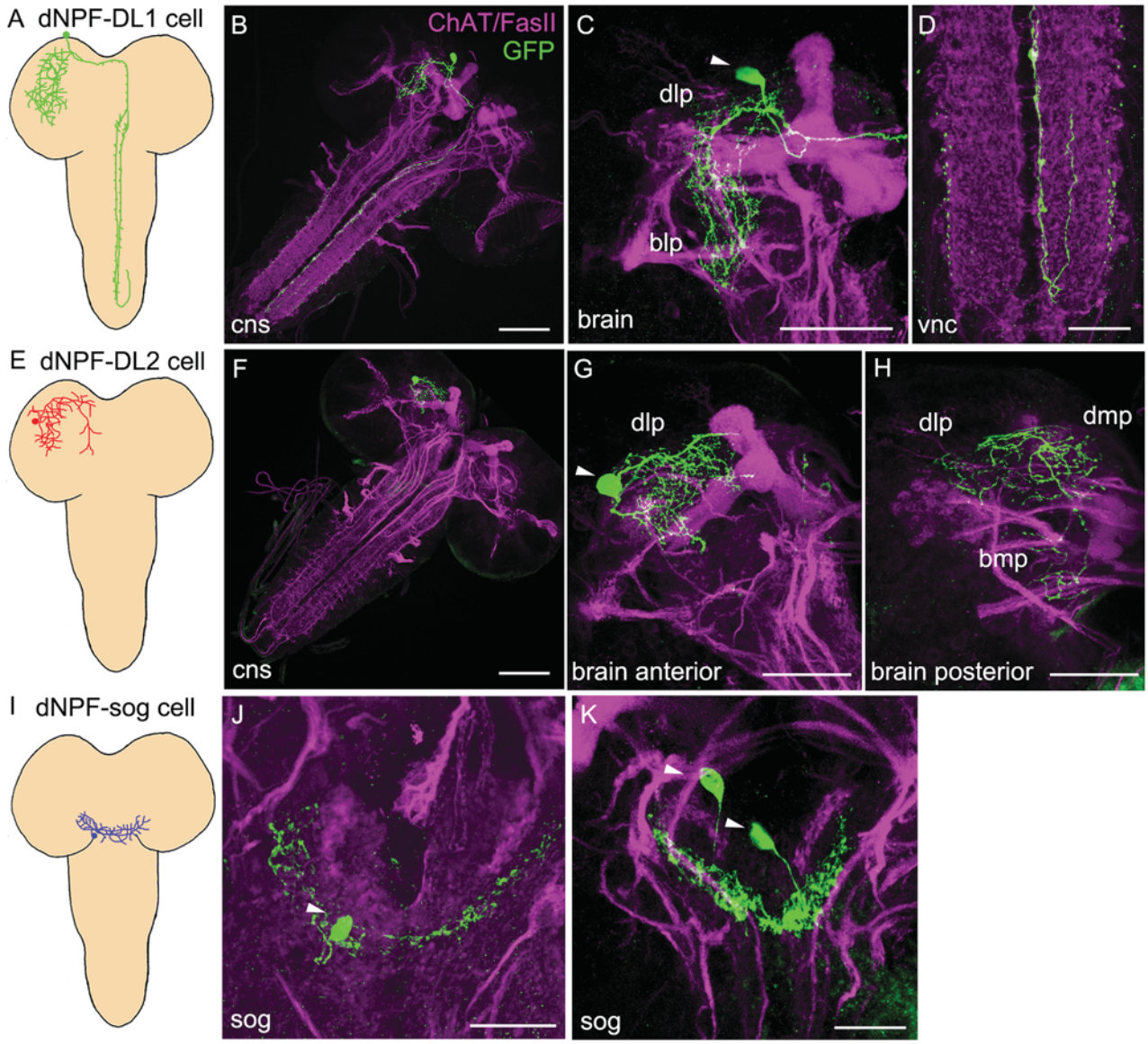

Figure 3. Single-cell organization of the dNPF circuit. Single-cell analysis of the larval dNPF neuronal circuit using the flp-out technique reveals three morphologically distinct types of cells per hemisphere. The different cell types are individually shown in green (GFP); in magenta the larval neuropil structure is shown. **A–D:** Morphology of the dNPF-DL1 cell type: (A) scheme of its neuronal organization. B–D: Detailed frontal view projections of the CNS, brain, and vnc, respectively. The position of the soma is indicated by an arrowhead in C. The dNPF-DL1 neuron gets input in the blp and dlp ipsilateral and sends a presynaptic arbor through the ipsilateral sog and vnc (see also Fig. 1G–J). **E–H:** Morphology of the dNPF-DL2 cell type: (E) scheme of its neuronal organization. F–H: Detailed frontal view projections of the CNS, brain, and vnc, respectively. The position of the soma is indicated by an arrowhead in G. The neuron has postsynaptic innervation mainly at the dlp and outputs basically at the dmp and bmp (see also Fig. 1G–J). **I–K:** Morphology of the dNPF-sog cell type: (I) scheme of its neuronal organization. J: Frontal view projection of the sog; dNPF-sog innervates the sog ipsi- and contralateral in a similar way. K: Double cell clone of the dNPF-sog cell type; cell bodies are indicated by arrowheads. The innervation patterns of both cells within the sog show a complete overlap. Scale bars = 50 µm in B,F; 25 µm in C,D,G,H,J,K.

sugar reward. Training is repeated three times. Immediately after training, in the test, the distribution of larvae between the sugar reward-paired odor and the unrewarded odor is measured. By comparing two groups that either are trained by rewarding odor A or odor B, a performance index reflecting associative olfactory learning can be calculated (Fig. 5A).

To test whether the dNPF system is necessary for larval olfactory learning we applied genetic techniques to interfere with dNPF neuronal function (Fig. 5B,E) but also on the dNPF receptor side (Fig. 5C,F). Both treatments did not reduce the naïve odor- or sugar-driven behavior of the experimental larva when compared to genetic controls (summarized in Table 2). First, using

dNPF-Gal4 we specifically ablated dNPF neurons by expressing the apoptosis-inducing genes *head involution defective (hid)* and *reaper (rpr)* (Thum et al., 2006; Pauls et al., 2015). The ablation was anatomically verified using an anti-dNPF antibody (Fig. 6). Second, we used a dNPF receptor mutant line (dNPFR1) that showed reduced performance after appetitive olfactory training in adult *Drosophila* (Krashes et al., 2009).

When trained with a low sugar reward of 0.02M fructose, control animals that harbor heterozygous only the dNPF-Gal4 or UAS-*hid,rpr* construct, showed significant learning above chance level ($P < 0.05$ for both groups; Fig. 5B). dNPF-Gal4/UAS-*hid,rpr* experimental animals, however, did not show a significant performance ($P > 0.05$; Fig. 5B). Similarly, dNPFR1 mutants did also not succeed in the learning task ($P > 0.05$; Fig. 5C) in

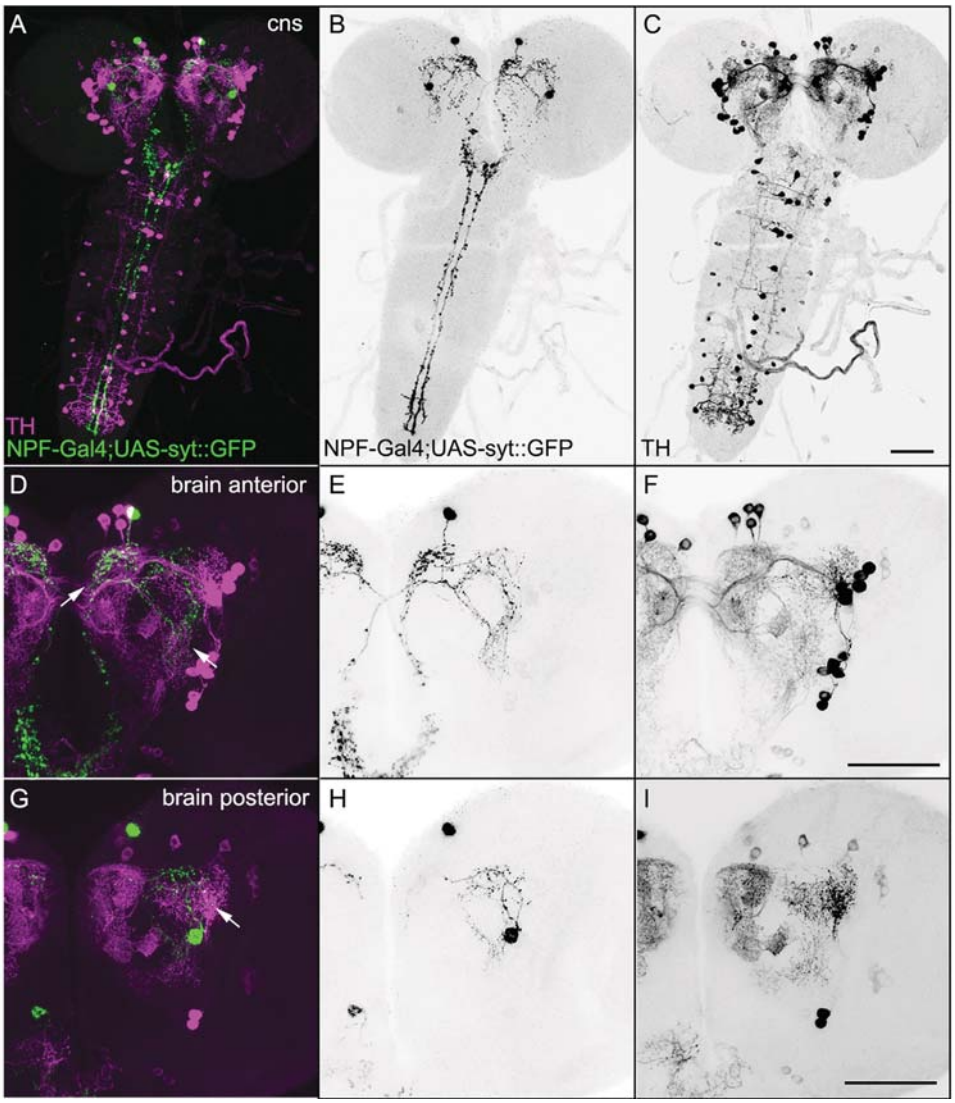

Figure 4. The dNPF overlaps with the dopaminergic and tyraminergic/octopaminergic neuronal circuits. **A–C:** Frontal view projections of dNPF-Gal4/UAS-*syt::GFP* larval brains double-labeled with anti-GFP (green) and anti-TH (tyrosine hydroxylase; magenta). The double labeling is shown for the entire central nervous system (A), the anterior part of a single brain hemisphere **(D)** and the posterior part of a single brain hemisphere **(G)**. **B,E,H:** Only the UAS-*syt::GFP* channel. **C,F,I:** Only the anti-TH labeling. Overlapping labeling of presynaptic structures of dNPF-Gal4-positive neurons and anti-TH was visible in the blp (arrow in D), in the dmp (arrow in B) and dlp (arrow in G). Only weak overlap was visible in the sog and vnc and other parts of the CNS. **J–R:** Frontal view projections of dNPF-Gal4/UAS-*syt::GFP* larval brains double-labeled with anti-GFP (green) and anti-TDC2 (tyrosine decarboxylase; magenta). The double labeling is shown for the entire central nervous system (J), the two brain hemispheres and the sog (M), and for a single brain hemisphere (P). K,N,Q: Only the UAS-*syt::GFP* channel. L,O,R: Only the anti-TDC2 labeling. Overlapping labeling of presynaptic structures of dNPF-Gal4-positive neurons and anti-TDC2 was visible mainly in the sog (arrow in M). In addition, weak overlap was detectable in the dmp and dlp (arrows in P). No overlap was visible in the vnc and other parts CNS. Scale bars = 50 μm in A–C, J–L; 25 μm in B–I, M–R.

http://doc.rero.ch

http://doc.rero.ch

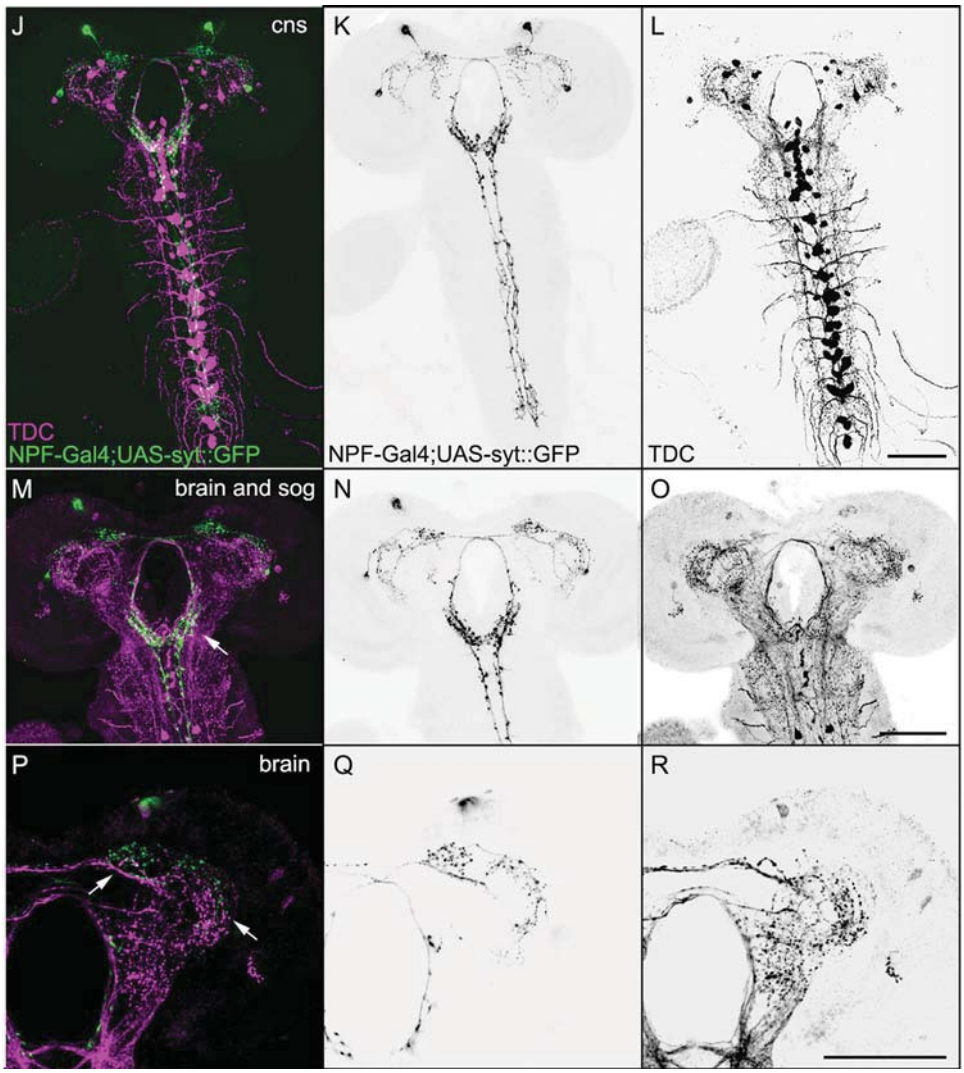

Figure 4. Continued

contrast to wildtype larvae that were able to associate an odor with 0.02M fructose reward ($P < 0.01$; Fig. 5C). However, note that in the ablation experiment we were not able to find a significant difference between the experimental group and both genetic controls.

When using a higher concentration of 2M fructose as a reward, both dNPF1-Gal4/UAS-*hid,rpr* and dNPFR1 mutant larvae showed significant olfactory learning ($P < 0.05$ and $P < 0.001$, respectively; Fig. 5E,F) similar to the behavioral responses of control larvae. Thus, we speculate that dNPF signaling is necessary for appetitive olfactory learning at a low concentration of 0.02M but dispensable at higher concentrations of 2M for *Drosophila* larvae under the conditions tested.

In addition, we also tested if appetitive olfactory conditioning depends on the feeding state of the larva (Fig. 5G–I) similar to effects reported for adult *Drosophila* (Krashes et al., 2009; Gruber et al., 2013). Neither wildtype larvae food deprived for 0, 60, or 180 minutes ($P < 0.01$ for 0 minutes and 180 minutes, $P < 0.001$ for 60 minutes, Fig. 5H), nor NPFR1 mutant larvae food deprived for 0 or 60 minutes behaved differently ($P < 0.001$ for 0 and 60 minutes, Fig. 5I). They all performed on a comparative level. Thus, under the conditions tested appetitive olfactory conditioning is independent of the feeding state of the early third instar larva.

Artificial activation of dNPF neurons impairs olfactory learning

Next, we analyzed if artificial activation of the dNPF neurons affects larval olfactory learning. For adult *Drosophila*, Krashes et al. (2009) reported that stimulation of dNPF neurons before testing increased the memory performance after appetitive olfactory learning in fed animals. In addition, Shohat-Ophir et al. (2012) found that dNPF neuron activation interferes with the ability

http://doc.rero.ch

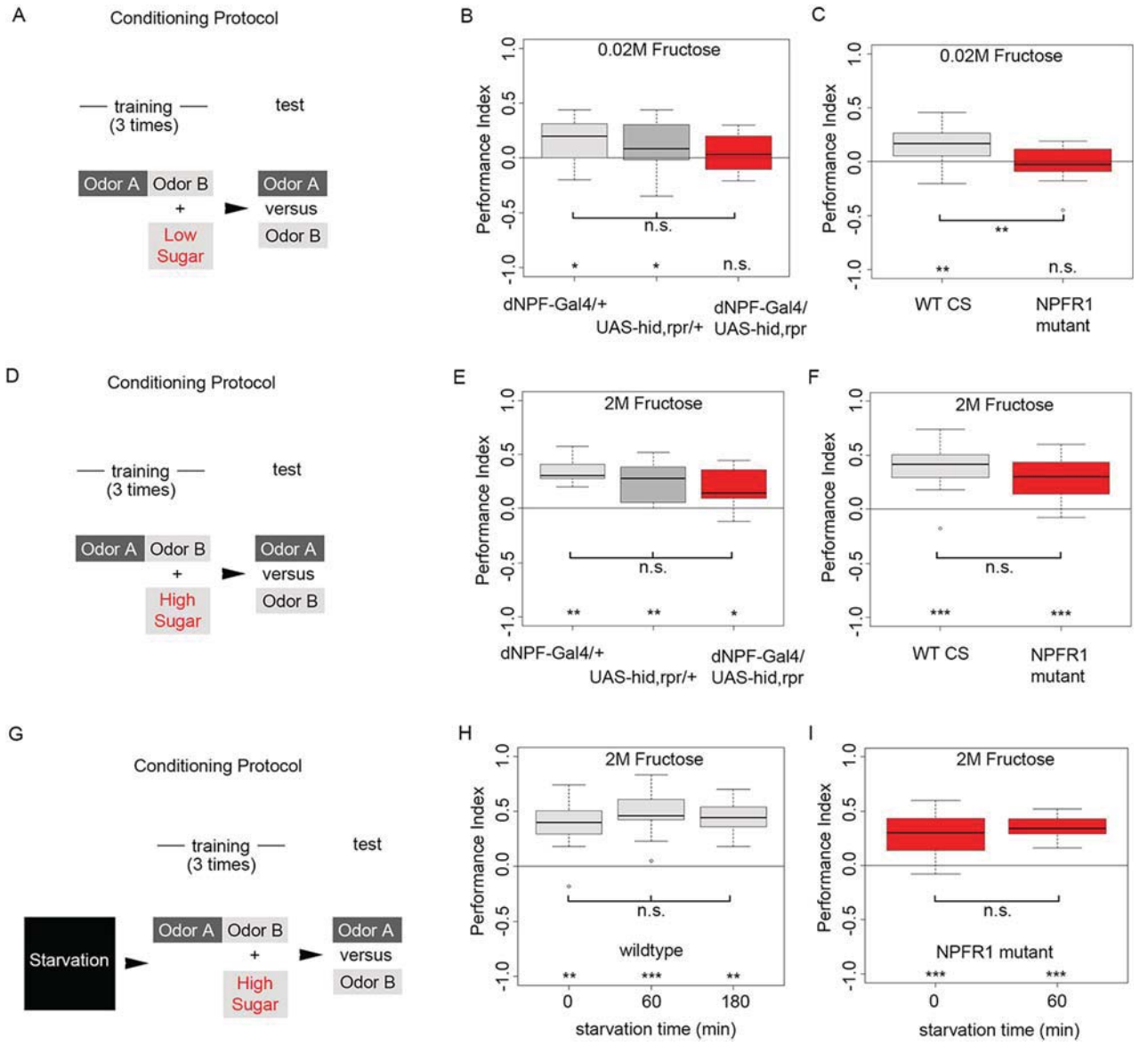

Figure 5. dNPF neuronal output is necessary for appetitive olfactory learning at low sugar concentrations. **A:** Procedural overview for appetitive olfactory conditioning using 0.02M fructose (low sugar) as a reward. **B:** Genetic ablation of dNPF-Gal4-positive neurons by expression of the cell death genes *head involution defective (hid)* and *reaper (rpr)* does impair odor-fructose learning reinforced with a low fructose concentration of 0.02M. **C:** A similar impairment for appetitive olfactory conditioning using 0.02M fructose was detectable for dNPF receptor mutants (NPFR1) that lack the receptor function of the dNPF signaling pathway. **D:** Procedural overview for appetitive olfactory conditioning using 2M fructose (high sugar) as a reward. **E:** Genetic ablation of the dNPF neuronal circuit does not affect appetitive olfactory conditioning using 2M sugar reinforcement. **F:** NPFR1 mutants are able to form appetitive olfactory associations after odor-2M fructose training. **G:** Procedural overview for appetitive olfactory conditioning using 2M fructose (high sugar) as a reward after starving larvae up to 180 minutes. **H:** Appetitive olfactory learning of wildtype larvae using 2M fructose reinforcement is not significantly different if tested without, after 60 minutes, and 180 minutes starvation. **I:** Appetitive olfactory learning of NPFR1 mutant larvae using 2M fructose reinforcement is not different if tested without or after 60 minutes starvation. Sample size for each box plot is $n > 12$. n.s. (not significant, $P > 0.05$), $^{*}P < 0.05$, $^{**}P < 0.01$, and $^{***}P < 0.001$. Significant differences between groups are shown for related boxplots. Significant differences for each group tested against random distribution are presented at the bottom of each boxplot.

of adult *Drosophila* to form odor-ethanol reward memory tested 24 hours after training, thus decreasing the memory performance.

In larvae, we either expressed the temperature-sensitive transient receptor potential channel A1 protein (TRPA1) that is required in a small number of neurons in the brain of *Drosophila* for temperature preference (Hamada et al., 2008). TRPA1 expressed in dNPF neurons conducts Ca^{2+} at temperatures of around 30°C, allowing a temperature-controlled activation of these neurons

http://doc.rero.ch

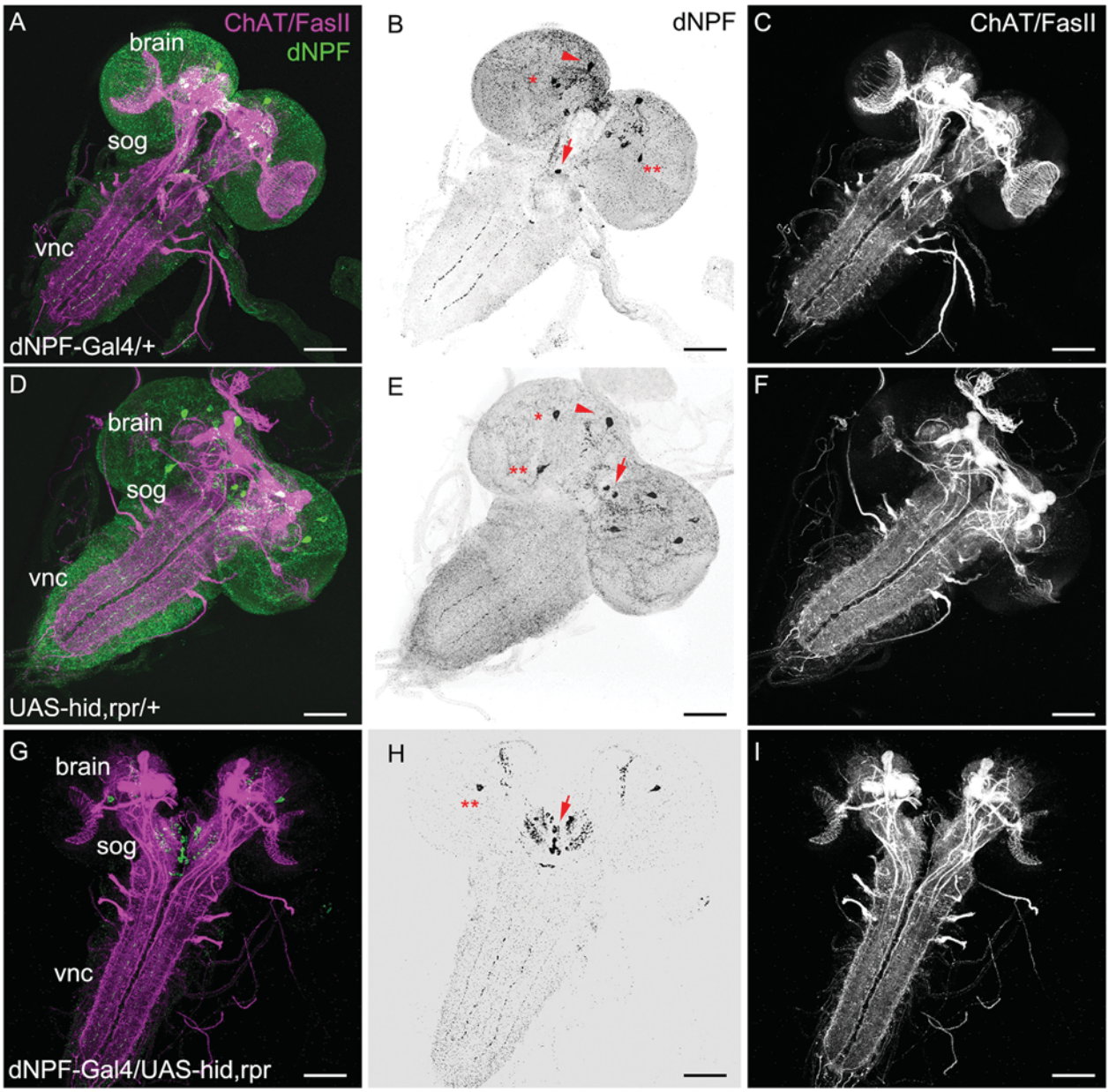

Figure 6. Expression of the cell death genes *head involution defective (hid)* and *reaper (rpr)* via dNPF-Gal4 ablates the related neuronal circuitry. All images show frontal view projections of complete larval central nervous systems labeled with anti-dNPF (green, first column; black, second column) and anti-ChAT/FasII (magenta, first column; white, third column). Thereby, visualization of dNPF-positive neurons within the neuropil region is possible. In the first column both channels are merged, whereas the second and third column shows each channel individually. **A–C:** Frontal brain view projections of genetic control larvae that harbor only the dNPF-Gal4 construct show anti-dNPF staining in a set of about 8–10 neurons in the CNS (red arrow, arrowhead, and asterisk). **D–F:** The same set of 8–10 neurons was also visualized in UAS-*hid,rpr* control larvae (red arrow, arrowhead, and asterisk). **G–I:** Frontal brain view projections of dNPF-Gal4/UAS-*hid,rpr* larvae suggest a successful ablation of most of the dNPF-Gal4-positive neurons. Yet two to four additional cells were detected in all samples in the hemispheres and the sog (two asterisks and arrow in E). The carboxyl structure of dNPF is highly conserved among a number of different neuropeptides. Thus, we assume that these cells are labeled due to cross reactivity of the antibody with other neuropeptides. Scale bars = 50 μm.

(Fig. 7A). Or alternatively, we expressed Channelrhodopsin-2 (ChR2), a blue light activated cation-selective ion channel (Fig. 7B–F) allowing for a temporally more precise light controlled activation of dNPF neurons (Schroll et al., 2006). The artificial activation of dNPF neurons by both techniques did not reduce the naïve behavior of the experimental larvae towards the olfactory and gustatory sensory stimuli when compared with both genetic

control groups (summarized in Table 2). (However, note that dNPF-Gal4;UAS-*TRPA1* experimental larvae were on a lower level than dNPF-Gal4 controls; yet they were not reduced compared to UAS-*TRPA1* effector control larvae).

Activation of dNPF neurons throughout training and test via TRPA1 strongly reduced olfactory learning of experimental larvae compared to both genetic controls ($P < 0.001$ compared to the UAS-control and $P < 0.01$ compared to the Gal4 control; Fig. 7A). To identify if the behavioral impairment upon dNPF neuron activation is specific for training, testing, or required in both, we used ChR2-dependent blue light activation limited to only one of the two phases. While activation of dNPF neurons during test does not change the learning performance compared to both controls ($P > 0.05$; Fig. 7C), there was a significant reduction specific for the training phase. dNPF-Gal4;UAS-*ChR2* larvae showed a reduced performance compared to both controls ($P < 0.001$ compared to the UAS-control and $P < 0.01$ compared to the Gal4 control; Fig. 7B). Taken together, these results suggest that dNPF neuron activation specifically affects the acquisition of an appetitive olfactory memory, where an odor stimulus is presented with sugar reward.

Artificial activation of dNPF neurons impairs unconditioned stimulus (US) processing

Is the decrease in learning success due to a decrease in the signal of the conditioned stimulus (CS, in our case odor) or of the unconditioned stimulus (US, in our case fructose)? The Rescorla-Wagner model for classical conditioning postulates that the value of the US is the limiting factor of the associative strength (Rescorla and Wagner, 1972). So if artificial dNPF neuron activation impairs the processing of the CS, the growth curve for memory formation with multiple training trials might be delayed but would reach asymptote at the same level as the appropriate control (Fig. 7E). In contrast, if artificial dNPF neuron activation diminishes the processing of the US, a lower US value might be associated with the CS stimuli, and the growth curve for memory formation with multiple training trials would reach asymptote at a lower level than the unimpaired control (Fig. 7F). The two different hypothetical curves (in red) are illustrated above Figure 7E,F compared to hypothetical wildtype larvae learning curves (in black) to provide a simple overview.

To test which of these possibilities is present in our case, we used a similar protocol as before (Fig. 7D). We activated dNPF neurons specifically during training but increased the number of training trials from one to three to five odor and sugar reward pairings. After one training trial all genotypes showed an appetitive learning score at a low level ($P < 0.05$; Fig. 7D). There was no significant difference between the experimental group and the controls ($P > 0.05$). After three training trials the performance indices of both control groups increased significantly compared to one training trial; yet for the experimental group this was not the case ($P > 0.05$; Fig. 7D,E). No further increase was seen with five training trials for both control groups, suggesting that already with three cycles a plateau in learning performance was reached (Fig. 7F) similar to results published by other labs (Neuser et al., 2005). Again, dNPF-Gal4/UAS-*ChR2* experimental larvae performed on a low level, even with five training trials ($P > 0.05$; Fig. 7D–F). Thus, artificial activation of the dNPF neurons likely reaches asymptote of the learning curve on a lower level, suggesting an impairment of the fructose US processing during training. Yet due to technical constraints it is not possible to further increase the number of training trials. Therefore, the interpretation of the results is limited.

Artificial activation of single dNPF neurons affects appetitive olfactory conditioning

Given the simplicity of the larval dNPF system that basically consists of only three pairs of neurons in the CNS, we next asked if it is possible to identify which of the three dNPF neurons mediates the observed phenotype. To this end, we used a technique recently established in adult *Drosophila* to stochastically activate TRPA1 function in single neurons of a given Gal4 pattern in different experimental animals (Fig. 8) (von Philipsborn et al., 2011).

In detail, we subjected UAS-*stop-myc::TRPA1; hs-flp,* dNPF-Gal4 experimental larvae to a brief heat shock of 6 minutes during embryonic development. By this, we could restrict myc::TRPA1 expression and function to only a single dNPF neuron (Fig. 8B). Next, we applied the following protocol: 1) heat activation of all experimental animals during olfactory conditioning; thus, artificial single cell activation of different dNPF neurons per animal (Fig. 8A); 2) separation of each individual larva into a learner or nonlearner after testing; 3) brain dissection of each individual larva; 4) immunohistochemical staining with an anti-myc antibody to label and identify the respective type of dNPF neuron in each brain; 5) confocal scanning of each brain to visualize the respective type of dNPF neuron in each brain sample (Fig. 8B). In total, we analyzed 299 larvae by correlating behavior (being a learner or a nonlearner) and single-cell anatomy (Fig. 8C). We calculated a single performance index for each dNPF cell type by

http://doc.rero.ch

subtracting the number of nonlearners from the learners divided by the sum of all tested larvae (therefore, no error bars in Fig. 8D). Activation of no cell did not affect appetitive odor-fructose learning and therefore serves as an internal control to exclude perturbing genetic and methodological effects (Fig. 8D). Activation of a single dNPF-DL1 and dNPF-DL2 neuron per hemisphere impaired larval odor-fructose learning. Activation of the dNPF-sog neuron type did not prevent experimental larvae from expressing a behavioral response; however, it was directed into the opposite direction, as most of the larvae avoided the fructose paired odor.

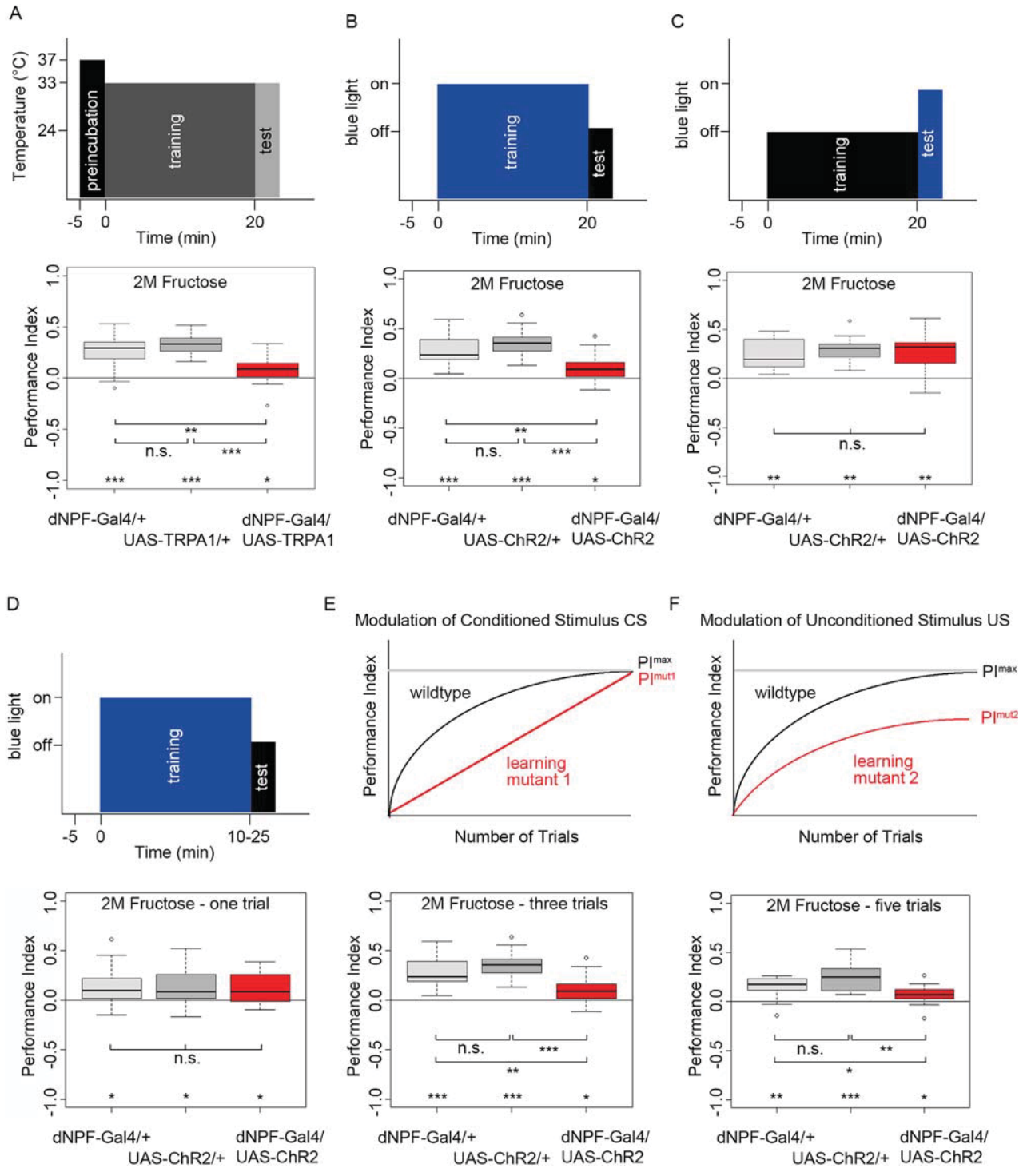

Figure 7.

http://doc.rero.ch

Thus, signaling per se was intact, but the hedonic value of the signal was inverted. Taken together, the data suggest that each type of dNPF cell is modulating the sugar reward signal on its own; either by reducing the reinforcing function of the fructose reward or by inverting the value of the sugar reward.

Artificial activation of dNPF neurons does not affect aversive olfactory learning

As artificial activation of dNPF neurons modulates fructose reward signaling, we next asked if this is also the case for punishment signaling. Therefore, we trained larvae with 1.5M sodium chloride that was reported to have a negative, aversive function during larval olfactory conditioning (Gerber and Hendel, 2006; Schleyer et al., 2011). We artificially activated dNPF neurons via blue light during training using ChR2. Here, dNPF-Gal4/UAS-*ChR2* experimental larvae performed on the same level as the two genetic control groups ($P > 0.05$; Fig. 9A). Thus, dNPF neuron activation specifically modulates sugar reward signaling but does not affect the processing of aversive, punishing stimuli under the conditions tested.

Artificial activation of dNPF neurons does not encode a reward itself

To test whether artificial activation of the dNPF neurons provides instructive reinforcement per se, we finally conducted a substitution experiment (Fig. 9B). In short, we conditioned larvae by presenting one odor paired with artificial ChR2-dependent dNPF neuron activation and a second odor without artificial activation (Schroll et al., 2006). Immediately after training, we tested if the larvae had established a preference towards the odor associated with artificial dNPF neuron activation. Experimental dNPF-Gal4/UAS-*ChR2* larvae and both genetic controls did not show a preference for the odor associated with blue light activation and performed all on the same level ($P > 0.05$; Fig. 9B). Thus, activation of the dNPF circuitry was not rewarding for larvae.

Manipulation of the neuronal activity of dNPF neurons does not change fructose-dependent feeding

Next we tested if interference with synaptic function of dNPF neurons changes larval feeding (Fig. 10). In short, we put 30 larvae on test plates that contained agarose, a blue dye, and 2M fructose. After 30 minutes the larvae were homogenized and the amount of ingested blue dye was measured photometrically (Rohwedder et al., 2012). In addition, we measured the amount of ingested food without the sugar stimulus to take apart general defects in feeding from the ones dependent on the fructose stimulus. Ablation of the dNPF-Gal4-positive neurons via UAS-*hid,rpr* significantly reduced the amount of consumed food compared to both genetic controls when tested on 2M fructose ($P < 0.05$; Fig. 10C). When tested on pure agarose no difference in the behavior was detectable ($P > 0.05$; Fig. 10B). In contrast, artificial activation of dNPF-Gal4-positive neurons via UAS-*TRPA1* during the entire test phase of 30 minutes (Fig. 10E,F) did not change the

Figure 7. Artificial activation of the dNPF neuronal circuitry impairs sugar reward processing of appetitive olfactory learning. **A:** Artificial activation of dNPF-Gal4-positive neurons during training and test by temperature induced TRPA1 function reduces odor-2M fructose learning. The effect is specific for the experimental group and cannot be seen in both genetic control groups. On top a scheme is shown that describes the used temperature regime that includes a 5-minute preincubation phase. **B,C:** A temporally more precise method of artificial dNPF neuron activation via blue light-induced ChR2 function allows to separate between training and test. Only when activated during training dNPF signaling impairs odor-fructose learning (B), whereas activation only during test has no effect (C). All genetic controls tested under these conditions show a comparable performance at a higher level. At the top a schematic overvie of the detailed blue light activation protocols is shown. **D,F:** Based on the Rescorla-Wagner model for classical conditioning the value of the unconditioned stimulus (US) is the limiting factor of the associative strength and therefore determines the final performance index (PI). Thus, if the conditioned stimulus (odor) is impaired by dNPF signaling, increasing the number of training trials would compensate for the lower acquisition rate (shown as a representative illustration in E at the top). The maximal PI^{mut1} for the experimental animals would reach the PI^{max}. If, however, US processing (sugar reward) is affected, increasing the number of training trials for the experimental animals would not lead to a PI^{mut2} at the wildtype level PI^{max} (shown as a representative illustration in F at the top). By this logic it is possible to separate between CS and US depending effects of dNPF neuronal signaling. D: After one training trial all tested groups showed a performance for appetitive olfactory learning at a lower level. E,F: After three and five training trials the performance indices of both control groups increased significantly compared to one training trial; yet for the experimental group this was not the case. Thus, we speculate that experimental animals reach the asymptote of the learning curve on a lower level, by that suggesting an impairment of the fructose reward processing during training. Sample size for each box plot is $n > 12$. n.s. (not significant $P > 0.05$), $^{*}P < 0.05$, $^{**}P < 0.01$, and $^{***}P < 0.001$. Significant differences between groups are shown for related boxplots. Significant differences for each group tested against random distribution are presented at the bottom of each boxplot.

http://doc.rero.ch

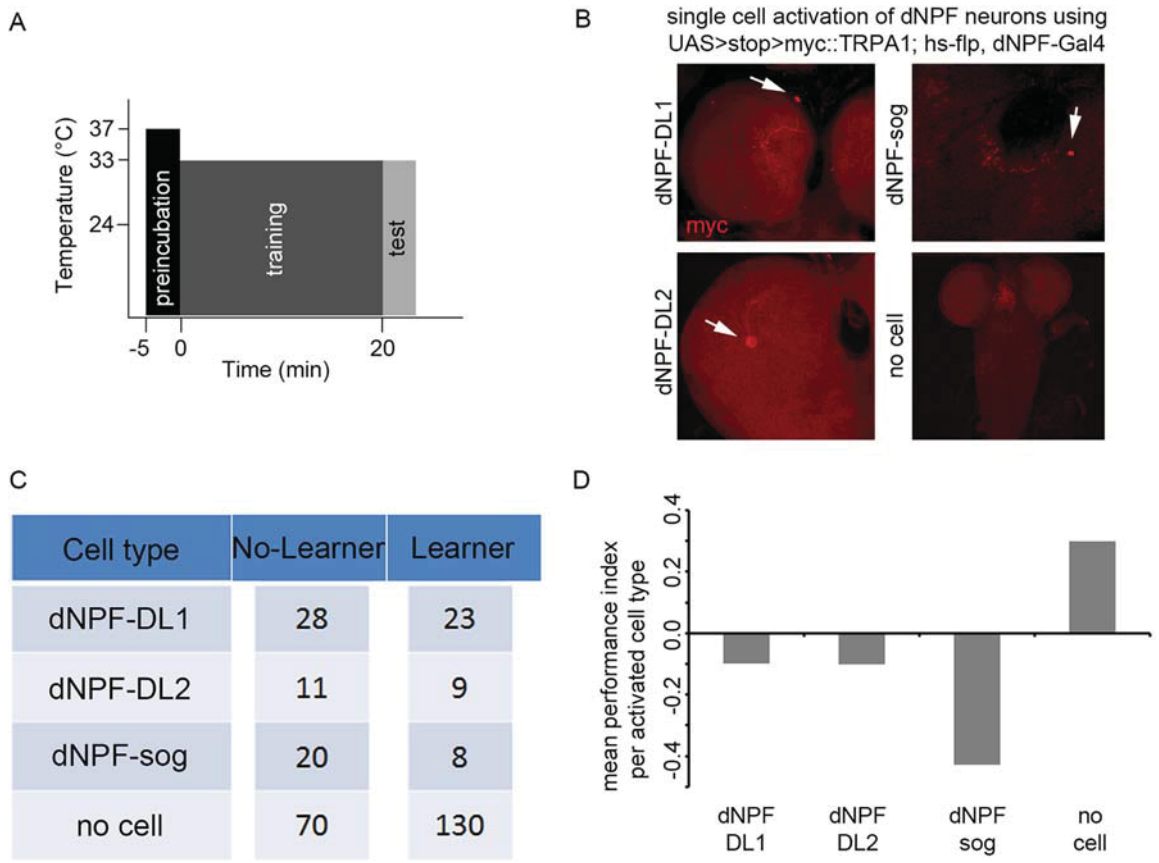

Figure 8. Artificial activation of single dNPF neurons impairs appetitive olfactory learning. **A:** An overview of the applied temperature activation protocol for appetitive olfactory conditioning and the subsequent test phase. **B:** Partial frontal view brain projections of different individuals. In each of the brains either, only a single dNPF-DL1 (top left), dNPF-DL2 (bottom left), dNPF-sog (top right), or no cell (bottom right) was labeled via anti-myc that recognizes a functional TRPA1 channel due to its myc tag. To obtain these results, dNPF-Gal4 was crossed to UAS>*stop*>*myc::TRPA1*; *hs-flp* flies. By applying a mild heat shock during embryonic development mostly single cell flp-out clones or no cell flp-out clones were generated. The identity of each flp-out event was tested anatomically by using an anti-myc staining for each individual brain after the behavioral test (schematically shown in A). **C:** 299 experimental larvae were behaviorally tested and classified as learner or nonlearner and based on the respective individual single cell labeling. **D:** By calculating a mean performance index per cell type it was possible to evaluate the function of each type of neuron for odor-fructose learning. Artificial activation of dNPF-DL1 or dNPF-DL2 abolished odor-fructose learning. Artificial activation of dNPF-sog did not abolish odor-fructose learning per se but rather changed the hedonic value of fructose from being rewarding to punishing. Activation of no cell was used as a genetic and methodological control to prove that odor-fructose learning was fine under the applied conditions.

amount of consumed food—independent of the presence or absence of fructose—when compared to both genetic control groups ($P > 0.05$; Fig. 10E,F). These results are in line with earlier work that showed that inactivation of the dNPF circuit leads to reduced feeding on glucose containing agar—potentially by being part of a postfeeding state signal (Cai and Shen, 2001; Wu et al., 2003). On the contrary, it was shown that activation of the dNPF circuit prolongs the feeding state or the motivation to consume noxious or cold food (Wu et al., 2003, 2005a,d). Yet it did not increase baseline feeding (Fig. 10). Thus, we assume that the above described effects on sugar reward learning (Figs. 1, 7, 8) are not based on different feeding levels in experimental and control larvae.

DISCUSSION

Neuronal circuit enabling larvae to associate odor information with sugar reward during classical conditioning

Drosophila larvae can learn to associate an odor with sugar taste reinforcement (Scherer et al., 2003; Honjo and Furukubo-Tokunaga, 2005; Neuser et al., 2005; Gerber and Hendel, 2006; Schleyer et al., 2011; Apostolopoulou et al., 2013). This implies convergence between the neuronal pathways signaling olfactory and sugar reinforcement information. Based on the simplicity and the genetic amenability of the larval nervous system, it was recently possible to establish a yet incomplete but nevertheless explicit neuronal circuit

http://doc.rero.ch

http://doc.rero.ch

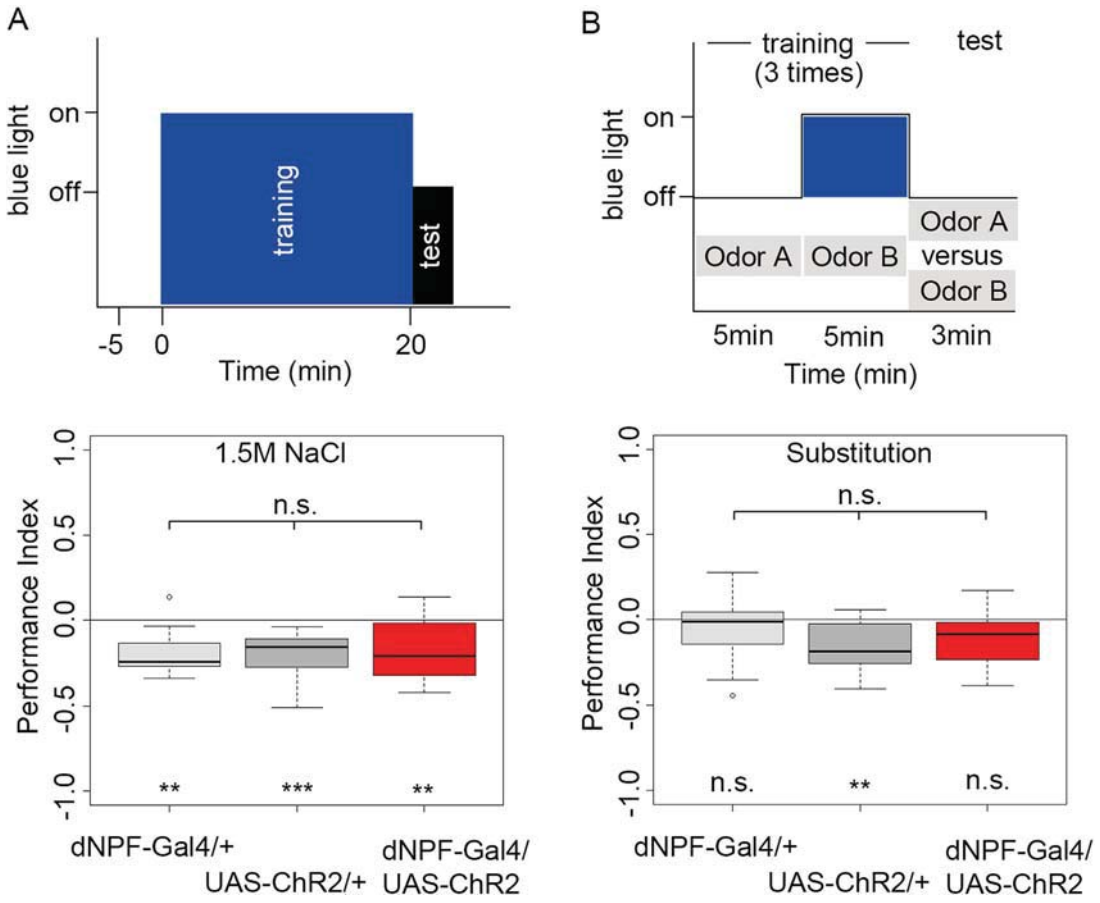

Figure 9. Artificial activation of dNPF neurons does not affect aversive olfactory learning and is not rewarding in itself. **A:** Aversive olfactory learning was tested using 1.5M NaCl as a negative reinforcer. Neuronal activity in dNPF-Gal4/UAS-*ChR2* experimental larvae was induced specifically during the training phase via artificial blue light activation (the detailed protocol is shown in A). Artificial activation of dNPF neurons does not affect aversive odor-salt learning as experimental larvae performed on the same level as both genetic controls ($P > 0.05$ when comparing each group in A). **B:** To test whether activation of the dNPF neurons is rewarding in itself, we applied a substitution protocol (shown at the top). Here, an odor is paired with the artificial ChR2-dependent blue light activation of the dNPF neurons instead of presenting a physical fructose reward. As a result dNPF-Gal4/UAS-*ChR2* larvae performed on the same level as both genetic controls ($P > 0.05$ when comparing each group). As none of the groups show a positive performance index, we suggest that dNPF neurons do not encode a rewarding function under the conditions tested. Sample size for each boxplot is $n > 12$. n.s. (not significant $P > 0.05$), $*P < 0.05$, $**P < 0.01$, and $***P < 0.001$. Significant differences between groups are shown for related boxplots. Significant differences for each group tested against random distribution are presented at the bottom of each boxplot.

underlying appetitive olfactory learning (reviewed in Gerber and Stocker, 2007; Schleyer et al., 2011). Here we identified an additional part of this circuit consisting of three pairs of dNPF neurons that specifically modulate sugar reinforcement signaling (Fig. 11).

What are the different identified layers of the larval "learning circuit" and what are their particular functions? How can the dNPF neurons be classified? Briefly summarized, one can distinguish between four different neuronal subcircuits (layers) that are fundamental for appetitive olfactory learning. The first subcircuit detects and processes olfactory information (Fig. 11, blue box), the second subcircuit detects and processes sugar reward (Fig. 11, yellow box), the third subcircuit receives input from both of these layers and offers a neuronal substrate to form appetitive olfactory associations (Fig. 11, green box), and finally the fourth subcircuit connects the memory center with premotor areas and motor neurons to ultimately trigger learned behavior (Fig. 11, gray box). Based on our results, we assume that the three pairs of dNPF neurons a part of the sugar reward signaling pathway (subcircuit two).

Subcircuit one: Olfactory information processing

Olfactory stimuli are sensed by only 21 ORNs housed in a single sensillum at the head of the larva, the dorsal organ–the unique olfactory sensory organ (Singh and

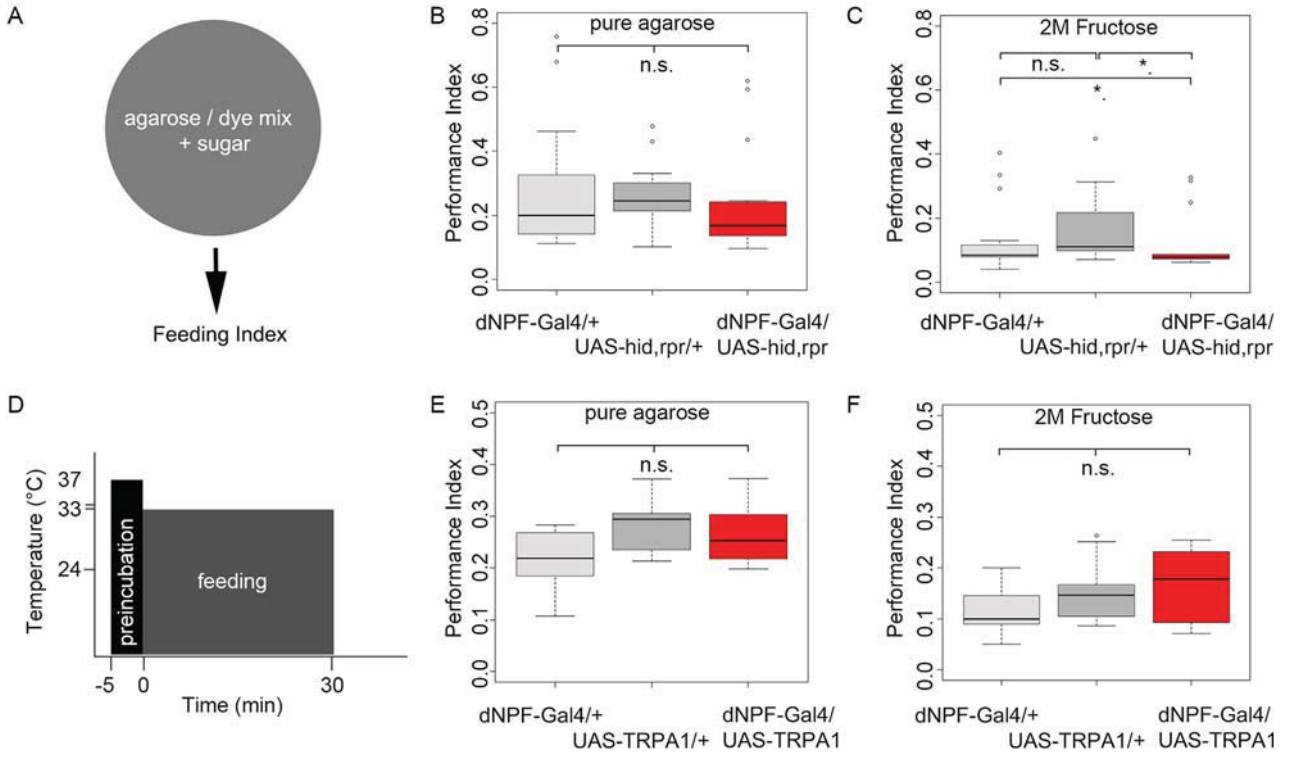

Figure 10. Genetic interference with dNPF neuronal signaling does not change the amount of food consumed over 30 minutes. **A:** Schematic overview of the experimental setup to test for larval feeding behavior. **B:** Feeding on pure agarose is not different in dNPF-Gal4/UAS-*hid,rpr* experimental larvae compared to its two genetic controls ($P > 0.05$). **C:** In contrast, ablation of dNPF-Gal4/UAS-*hid,rpr* larvae reduces the amount of consumed food compared to both genetic controls ($P < 0.05$). **D:** Schematic overview of the temperature regime to test if artificial activation of dNPF-Gal4-positive neurons via UAS-*TRPA1* changes the amount of consumed food within 30 minutes. **E:** Artificial activation of dNPF-Gal4-positive neurons during the experiment does not change larval feeding behavior on pure agarose substrate. dNPF-Gal4/UAS-*TRPA1* experimental larvae consumed the same amount of food as two genetic control groups ($P > 0.05$). **F:** Temperature-induced artificial activation of the dNPF-Gal4-positive neurons via UAS-*TRPA1* did not change feeding of experimental larvae on 2M fructose when compared to the genetic controls ($P > 0.05$). Sample size for each box plot is $n > 12$. n.s. (not significant $P > 0.05$) and $^*P < 0.05$.

Singh, 1984; Oppliger et al., 2000; Python and Stocker, 2002; Fishilevich et al., 2005; Kreher et al., 2005). The olfactory information from a given ORN is further conveyed by nearly exclusively one PN to the lateral horn and the calyx region of the MB (Ramaekers et al., 2005; Masuda-Nakagawa et al., 2009, 2010; Thum et al., 2011) (Fig. 11, blue box).

Based on our results we exclude an involvement of dNPF neurons in olfactory information processing: 1) The six dNPF neurons are not anatomically linked with first-, second-, and third-order olfactory neurons (Fig. 1–3). 2) Artificial activation and inactivation of dNPF-positive neurons does not change the naïve response of the experimental larvae towards the two odors tested (Table 2). 3) Aversive olfactory learning is not impaired by artificial activation of the dNPF-positive neurons and thus suggests a proper processing of odor information (Fig. 9A). 4) Artificial activation of the dNPF-positive neurons only during test does not reduce the odor-fructose learning (Fig. 7C). Thus, odor information processing has to be independent of dNPF neuron activation.

Subcircuit two: Sugar reinforcement processing

Drosophila larvae perceive gustatory stimuli via three external chemosensory organs located on the head and three internal organs located along the pharynx (Singh and Singh, 1984; Python and Stocker, 2002). The six sensory organs house about 90 GRNs and transfer taste information from the periphery to the sog—the first-order taste center of the larval brain (Python and Stocker, 2002; Colomb et al., 2007; Kwon et al., 2011; Mishra et al., 2013). Yet our knowledge on larval sugar sensors remains limited and additional mechanisms recently proposed for *Drosophila* and honeybees may contribute (Ayestaran et al., 2010; Wright et al., 2010; Miyamoto et al., 2012; Dus et al., 2013; Gruber et al., 2013).

http://doc.rero.ch

http://doc.rero.ch

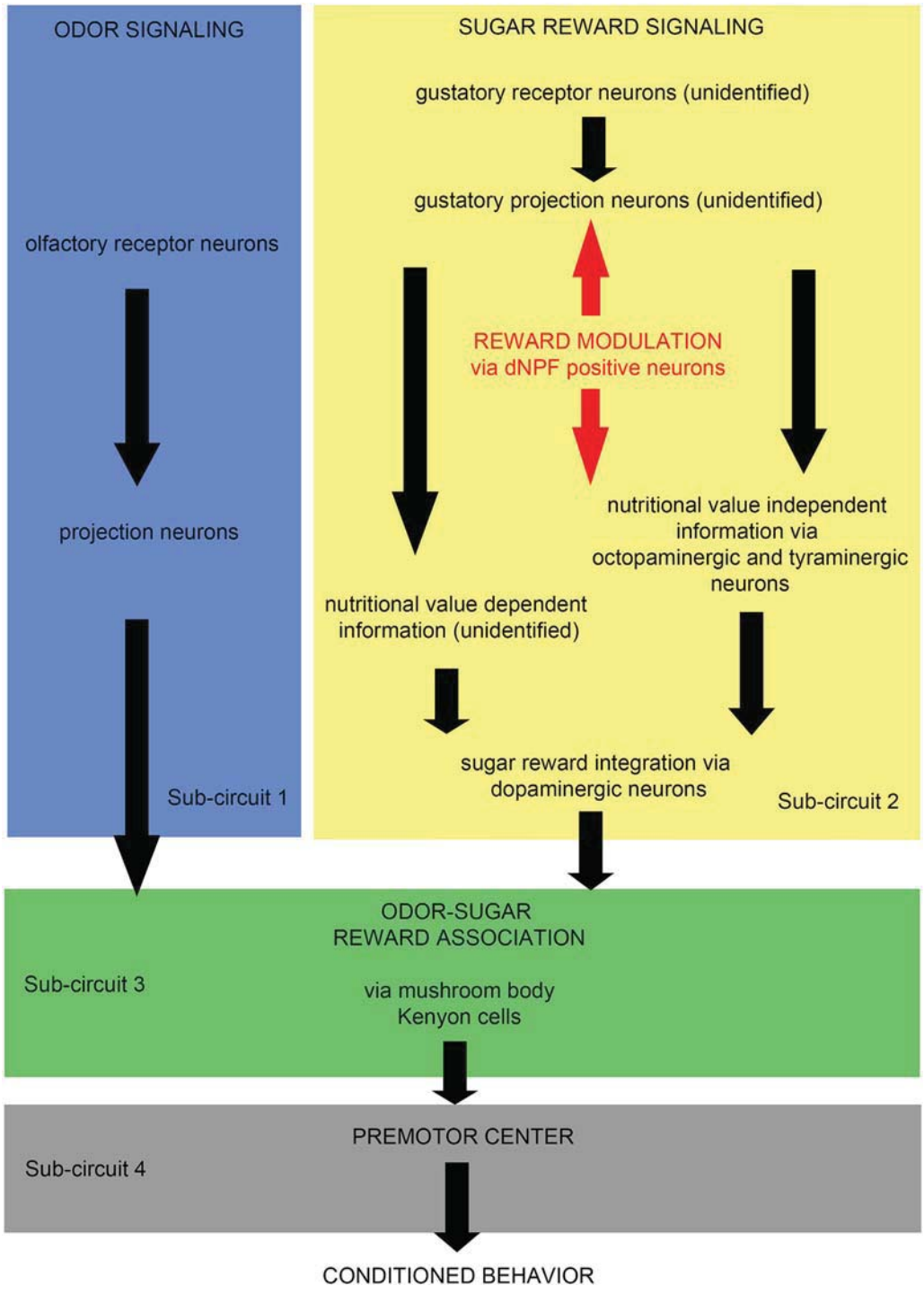

Figure 11. A simplified neuronal circuit essential for appetitive olfactory learning in *Drosophila* larvae. The depicted neuronal circuit summarizes the neurons that were reported to be involved appetitive olfactory learning. Basically, four different neuronal subcircuits can be distinguished for the entire circuit. The first subcircuit detects and processes olfactory information (blue box) via 21 olfactory receptor neurons from the dorsal organ to the antennal lobe. From here, about 21 projection neurons further signal the information to the mushroom body. The second subcircuit detects and processes sugar reward (yellow box). Sugar reward signals consist of a nutritional value-dependent information (unknown neuronal substrate) and nutritional value independent information (signaled by octopaminergic and tyraminergic neurons). Both types of information are integrated by dopaminergic neurons that form the most downstream part of this subcircuit. The third subcircuit receives input from both sensory modalities and offers a neuronal substrate to form an association between the olfactory stimulus and the sugar reward (green box). A comprehensive set of experiments suggest that the mushroom body Kenyon cells form subcircuit three. The fourth subcircuit connects the memory center with premotor areas and motor neurons to ultimately trigger learned behavior (gray box); its neuronal substrate is to date largely unknown. Based on the results presented here, we assume that the three pairs of dNPF neurons belong modulate the sugar reward signal and thus are part of subcircuit two.

In contrast, DA and OA/TA neurons are obviously involved in sugar reinforcement signaling. Sugar reinforcement includes nutrition-dependent and nutrition-independent information (Fujita and Tanimura, 2011; Burke et al., 2012; Rohwedder et al., 2012). The DA system integrates both types of information since DA neurons as well as the dopamine receptor dDA1 are required for odor-fructose learning (fructose is perceived as nutritious and sweet by the larva) (Selcho et al., 2009; Rohwedder et al., 2012). DA neurons directly output onto the MB lobes and consequently form the most downstream element of the sugar reinforcing subcircuit (Fig. 11). Activation of OA/TA neurons–likely upstream of the DA system–is sufficient to replace the sugar reward during appetitive olfactory conditioning (Schroll et al., 2006). In addition, neuronal activation of OA/TA neurons is necessary during appetitive olfactory conditioning to establish short lasting appetitive olfactory memories up to 60 minutes (Honjo and Furukubo-Tokunaga, 2009) or odor-arabinose sugar memories (a sugar that is attractive to larvae but offers no nutritional benefit) (Rohwedder et al., 2012; Selcho et al., 2014). Yet in contrast to adult *Drosophila*, the synaptic connection of OA/TA neurons onto DA was not functionally verified and therefore remains purely hypothetical (Fig. 11, yellow box).

In adult *Drosophila*, it was shown that DA neurons of the PAM cluster downstream of OA/TA neurons project on the mushroom body and signal sweet-only information through the adrenergic OAMB receptor (Burke et al., 2012; Huetteroth et al., 2015). Distinct reinforcing DA neurons in the PAM cluster were found to relay water reward in an OA-independent manner (Lin et al., 2014) and other DA subtypes in the PAM cluster signal the nutritional value of sugar reward (Huetteroth et al., 2015; Yamagata et al., 2015). Artificially stimulating any of these DA neurons paired with odor presentation implants memories which differ in their time course (Burke et al., 2012; Liu et al., 2012; Lin et al., 2014; Huetteroth et al., 2015; Yamagata et al., 2015).

Subcircuit two: Three pairs of dNPF neurons

Based on the anatomical and behavioral results of our study we conclude that the three pairs of dNPF neurons can be assigned to the sugar reward processing circuit. Consequently, our results expand subcircuit two that consists so far of about 14 DA neurons and 39 OA/TA neurons by three pairs of dNPF neurons (Selcho et al., 2009, 2014). Our conclusion is based on the following results: First, dNPF neurons overlap in the dmp, dlp and blp (Fig. 4A–I) with dopaminergic neurons that form the most downstream element of the sugar reinforcing subcircuit (Selcho et al., 2009; Burke et al., 2012; Liu et al., 2012). Second, dNPF neurons and NPFR1 are required for sugar reward learning using lower concentrations (Fig. 5B,C). Third, at higher concentrations artificial activation of dNPF neurons impairs appetitive olfactory learning (Fig. 7A). The impairment relates exclusively to the training phase (Fig. 7B), it specifically impairs the processing of the sugar reward (Fig. 7D–F). Fourth, artificial activation of individual dNPF neurons either impairs appetitive olfactory learning or changes the conditioned response from attraction to avoidance (Fig. 8).

Subcircuit three: The mushroom body harbors a memory trace

Several findings suggest that the MBs harbor a memory trace after appetitive olfactory conditioning in larvae (Fig. 11). Different studies suggest that 1) neuronal plasticity occurs in these larval MB Kenyon cells (Crittenden et al., 1998; Honjo and Furukubo-Tokunaga, 2005); 2) neuronal output of the MB Kenyon cells–specifically during test–is necessary for appetitive olfactory conditioning (Honjo and Furukubo-Tokunaga, 2005; Pauls et al., 2010); 3) the larval MB function is sufficient for appetitive olfactory conditioning (Kaun et al., 2007; Michels et al., 2011). Thus, it was concluded that the subcircuit consists of only a small subset of about 100 embryonic-born MB Kenyon cells (Pauls et al., 2010; Michels et al., 2011). In line with this model, our findings exclude any involvement of the larval dNPF neurons in this layer of the learning network (Fig. 11).

Subcircuit four: Premotor centers triggering conditioned behavior

The simple nervous system of the *Drosophila* larva is able to generate many distinct motor patterns (Vogelstein et al., 2014; Ohyama et al., 2015). However, our current knowledge of the neuronal circuits downstream of the larval MB "memory center" that triggers motor patterns to drive learned behavior is very limited. A yet purely anatomical evaluation suggests that only a small set of MB output neurons exists (likely around 30 neurons per hemisphere) (Pauls et al., 2010) similar to adult *Drosophila* and potentially also to honeybees (Mauelshagen, 1993; Okada et al., 2007; Aso et al., 2014a,b). Other types of neurons that might contribute to this subcircuit are so far unknown (excluding motor neurons).

Our findings also exclude an involvement of dNPF neurons in subcircuit four. We argue that artificial activation or inactivation of dNPF neurons does not alter different behavioral outputs of the larvae, including

http://doc.rero.ch

naïve olfactory and gustatory-driven responses (Table 2), aversive olfactory conditioning (Fig. 9A), and feeding (Fig. 10). Thus, it is unlikely that dNPF neurons act downstream of the MB onto premotor areas to modulate appetitive olfactory learning.

OUTLOOK

How do the results presented here influence the future analysis of the sugar reward signaling circuit? Single-cell activation of the dNPF-sog cell leads to a sign inversion of the learning, whereas either activation of the dNPF-DL1 or the dNPF-DL2 neuron or of all dNPF neurons reduces odor-fructose learning (Figs. 7, 8). This suggests that the dNPF neurons are linked with the larval reward circuit at multiple levels, potentially including the sog, the dmp, and on a lower level the dlp.

The sog receives information from about 90 mainly gustatory sensory neurons located at the larval head. The enteric nervous system, which has been shown in insects to be important for taste-dependent behaviors, projects in addition to the sog (Penzlin, 1985; Spiess et al., 2008; Schoofs et al., 2014). Therefore, the sog forms the first-order gustatory center of the larval brain and collects from several internal and external sensory organs gustatory cues to process different types of food-related information (Singh and Singh, 1984; Python and Stocker, 2002; Wu et al., 2003, 2005a,d; Colomb et al., 2007; Kwon et al., 2011). Yet in larvae the nature of the sensory neurons that instruct the rewarding function is completely unknown and an involvement of the sog in appetitive olfactory learning was not described. Given the sign inversion after dNPF-sog activation we provide such evidence for the first time. Thus future research will include new sets of available Gal4 lines to identify the sensory neurons that are involved in reward signaling and project to the sog (Kwon et al., 2011; Mishra et al., 2013; Li et al., 2014; Stewart et al., 2015).

Artificial activation of the dNPF-DL2 neuron reduces odor-fructose learning (Fig. 8) and the effect is dominant over the dNPF-sog neuron-dependent sign inversion when all dNPF-Gal4 neurons are activated in combination. This suggests a more downstream function of the dNPF-DL2 neuron in the reward pathway than for the dNPF-sog neuron. The morphology of the dNPF-DL2 neuron is limited to one brain hemisphere and clearly excludes the sog. Its output is limited mainly to the dmp (Figs. 1–3). Thus, we suggest that—in addition to the sog—the dmp is also involved in sugar reward signaling. Indeed, the dmp is innervated by 11 DA neurons and four OA/TA neurons (Selcho et al., 2009, 2014). Both sets of neurons were shown to be involved in appetitive olfactory learning (Honjo and Furukubo-Tokunaga, 2009; Selcho et al., 2009, 2014). Hence, it seems promising to further focus on the DA, TA/OA, dNPF circuit and their upstream partners in dmp when reconstructing the neuronal circuit that encodes sugar reward in the *Drosophila* larval brain.

ACKNOWLEDGMENTS

We thank Prof. Reini Stocker and Dr. Dennis Pauls for their fruitful comments on the article. Additionally, we thank Lyubov Pankevych and Margarete Ehrenfried for fly care and maintenance of the wildtype Canton-S stock. We especially acknowledge the Shen, Waddell, Heisenberg, Sprecher, Dickson, Struhl, and Neckameyer lab for fly strains and antibodies. The anatomical work was supported by the Bioimaging Facility of the University of Konstanz.

CONFLICT OF INTEREST

The authors declare no competing interests.

ROLE OF THE AUTHORS

All authors had full access to all the data in the study and take responsibility for the integrity of the data and the accuracy of the data analysis. Study concept and design: AR, MS, and AST. Acquisition of data: AR, MS, and BC. Analysis, and interpretation of data: AR, MS, BC, and AST. Drafting of the article: AR, MS, and AST. Critical revision of the article for important intellectual content: AR, MS, BC, and AST. Statistical analysis: AR, BC, and AST. Obtained funding: AST. Study supervision: AR, MS, BC, and AST.

LITERATURE CITED

Apostolopoulou AA, Widmann A, Rohwedder A, Pfitzenmaier JE, Thum AS. 2013. Appetitive associative olfactory learning in Drosophila larvae. J Vis Exp JoVE (72) pii 4334.

Apostolopoulou AA, Mazija L, Wust A, Thum AS. 2014. The neuronal and molecular basis of quinine-dependent bitter taste signaling in Drosophila larvae. Front Behav Neurosci 8:6.

Aso Y, Hattori D, Yu Y, Johnston RM, Iyer NA, Ngo TT, Dionne H, Abbott L, Axel R, Tanimoto H, Rubin GM. 2014a. The neuronal architecture of the mushroom body provides a logic for associative learning. eLife 3.

Aso Y, Sitaraman D, Ichinose T, Kaun KR, Vogt K, Belliart-Guerin G, Placais PY, Robie AA, Yamagata N, Schnaitmann C, Rowell WJ, Johnston RM, Ngo TT, Chen N, Korff W, Nitabach MN, Heberlein U, Preat T, Branson KM, Tanimoto H, Rubin GM. 2014b. Mushroom body output neurons encode valence and guide memory-based action selection in Drosophila. eLife 3.

Ayestaran A, Giurfa M, de Brito Sanchez MG. 2010. Toxic but drank: gustatory aversive compounds induce post-ingestional malaise in harnessed honeybees. PLoS One 5:e15000.

http://doc.rero.ch

http://doc.rero.ch

Beck B. 2001. KO's and organisation of peptidergic feeding behavior mechanisms. Neurosci Biobehav Rev 25:143–158.

Bidaye SS, Machacek C, Wu Y, Dickson BJ. 2014. Neuronal control of Drosophila walking direction. Science 344:97–101.

Brown MR, Crim JW, Arata RC, Cai HN, Chun C, Shen P. 1999. Identification of a Drosophila brain-gut peptide related to the neuropeptide Y family. Peptides 20:1035–1042.

Burke CJ, Huetteroth W, Owald D, Perisse E, Krashes MJ, Das G, Gohl D, Silies M, Certel S, Waddell S. 2012. Layered reward signalling through octopamine and dopamine in Drosophila. Nature 492:433–437.

Cai HN, Shen P. 2001. Effects of cis arrangement of chromatin insulators on enhancer-blocking activity. Science 291: 493–495.

Colomb J, Grillenzoni N, Ramaekers A, Stocker RF. 2007. Architecture of the primary taste center of Drosophila melanogaster larvae. J Comp Neurol 502:834–847.

Crittenden JR, Skoulakis EM, Han KA, Kalderon D, Davis RL. 1998. Tripartite mushroom body architecture revealed by antigenic markers. Learn Mem 5:38–51.

Dierick HA, Greenspan RJ. 2007. Serotonin and neuropeptide F have opposite modulatory effects on fly aggression. Nat Genet 39:678–682.

Dus M, Ai M, Suh GS. 2013. Taste-independent nutrient selection is mediated by a brain-specific Na+ /solute co-transporter in Drosophila. Nat Neurosci 16:526–528.

Dyzma M, Boudjeltia KZ, Faraut B, Kerkhofs M. 2010. Neuropeptide Y and sleep. Sleep Med Rev 14:161–165.

Farris SM. 2013. Evolution of complex higher brain centers and behaviors: behavioral correlates of mushroom body elaboration in insects. Brain Behav Evol 82:9–18.

Fishilevich E, Domingos AI, Asahina K, Naef F, Vosshall LB, Louis M. 2005. Chemotaxis behavior mediated by single larval olfactory neurons in Drosophila. Curr Biol 15: 2086–2096.

Fujita M, Tanimura T. 2011. Drosophila evaluates and learns the nutritional value of sugars. Curr Biol 21:751–755.

Gerber B, Hendel T. 2006. Outcome expectations drive learned behaviour in larval Drosophila. Proc Biol Sci R Soc 273:2965–2968.

Gerber B, Stocker RF. 2007. The Drosophila larva as a model for studying chemosensation and chemosensory learning: a review. Chem Senses 32:65–89.

Gonzalez R, Orchard I. 2008. Characterization of neuropeptide F-like immunoreactivity in the blood-feeding hemipteran, Rhodnius prolixus. Peptides 29:545–558.

Grenningloh G, Rehm EJ, Goodman CS. 1991. Genetic analysis of growth cone guidance in Drosophila: fasciclin II functions as a neuronal recognition molecule. Cell 67:45–57.

Gruber F, Knapek S, Fujita M, Matsuo K, Bracker L, Shinzato N, Siwanowicz I, Tanimura T, Tanimoto H. 2013. Suppression of conditioned odor approach by feeding is independent of taste and nutritional value in Drosophila. Curr Biol 23:507–514.

Hamada FN, Rosenzweig M, Kang K, Pulver SR, Ghezzi A, Jegla TJ, Garrity PA. 2008. An internal thermal sensor controlling temperature preference in Drosophila. Nature 454:217–220.

Hamasaka Y, Suzuki T, Hanai S, Ishida N. 2010. Evening circadian oscillator as the primary determinant of rhythmic motivation for Drosophila courtship behavior. Genes Cells 15:1240–1248.

Heisenberg M. 2003. Mushroom body memoir: from maps to models. Nat Rev Neurosci 4:266–275.

Hilpert K, Hansen G, Wessner H, Kuttner G, Welfle K, Seifert M, Hohne W. 2001. Anti-c-myc antibody 9E10: epitope key positions and variability characterized using peptide spot synthesis on cellulose. Protein Eng 14:803–806.

Honjo K, Furukubo-Tokunaga K. 2005. Induction of cAMP response element-binding protein-dependent medium-term memory by appetitive gustatory reinforcement in Drosophila larvae. J Neurosci 25:7905–7913.

Honjo K, Furukubo-Tokunaga K. 2009. Distinctive neuronal networks and biochemical pathways for appetitive and aversive memory in Drosophila larvae. J Neurosci 29:852–862.

Huetteroth W, Perisse E, Lin S, Klappenbach M, Burke C, Waddell S. 2015. Sweet taste and nutrient value subdivide rewarding dopaminergic neurons in Drosophila. Curr Biol 25:751–758.

Kalra SP, Crowley WR. 1992. Neuropeptide Y: a novel neuroendocrine peptide in the control of pituitary hormone secretion, and its relation to luteinizing hormone. Front Neuroendocrinol 13:1–46.

Kaun KR, Hendel T, Gerber B, Sokolowski MB. 2007. Natural variation in Drosophila larval reward learning and memory due to a cGMP-dependent protein kinase. Learn Mem 14:342–349.

Keene AC, Waddell S. 2007. Drosophila olfactory memory: single genes to complex neural circuits. Nat Rev Neurosci 8:341–354.

Kim YC, Lee HG, Han KA. 2007. D1 dopamine receptor dDA1 is required in the mushroom body neurons for aversive and appetitive learning in Drosophila. J Neurosci 27: 7640–7647.

Kim YC, Lee HG, Lim J, Han KA. 2013. Appetitive learning requires the alpha1-like octopamine receptor OAMB in the Drosophila mushroom body neurons. J Neurosci 33: 1672–1677.

Krashes MJ, DasGupta S, Vreede A, White B, Armstrong JD, Waddell S. 2009. A neural circuit mechanism integrating motivational state with memory expression in Drosophila. Cell 139:416–427.

Kreher SA, Kwon JY, Carlson JR. 2005. The molecular basis of odor coding in the Drosophila larva. Neuron 46:445–456.

Kurada P, White K. 1998. Ras promotes cell survival in Drosophila by downregulating hid expression. Cell 95:319–329.

Kwon JY, Dahanukar A, Weiss LA, Carlson JR. 2011. Molecular and cellular organization of the taste system in the Drosophila larva. J Neurosci 31:15300–15309.

Lee T, Luo L. 1999. Mosaic analysis with a repressible cell marker for studies of gene function in neuronal morphogenesis. Neuron 22:451–461.

Lee G, Bahn JH, Park JH. 2006. Sex- and clock-controlled expression of the neuropeptide F gene in Drosophila. Proc Natl Acad Sci U S A 103:12580–12585.

Li XJ, Wu YN, North RA, Forte M. 1992. Cloning, functional expression, and developmental regulation of a neuropeptide Y receptor from Drosophila melanogaster. J Biol Chem 267:9–12.

Li HH, Kroll JR, Lennox SM, Ogundeyi O, Jeter J, Depasquale G, Truman JW. 2014. A GAL4 driver resource for developmental and behavioral studies on the larval CNS of Drosophila. Cell Rep 8:897–908.

Lin S, Owald D, Chandra V, Talbot C, Huetteroth W, Waddell S. 2014. Neural correlates of water reward in thirsty Drosophila. Nat Neurosci 17:1536–1542.

Liu C, Placais PY, Yamagata N, Pfeiffer BD, Aso Y, Friedrich AB, Siwanowicz I, Rubin GM, Preat T, Tanimoto H. 2012. A subset of dopamine neurons signals reward for odour memory in Drosophila. Nature 488:512–516.

Masuda-Nakagawa LM, Gendre N, O'Kane CJ, Stocker RF. 2009. Localized olfactory representation in mushroom bodies of Drosophila larvae. Proc Natl Acad Sci U S A 106:10314–10319.

Masuda-Nakagawa LM, Awasaki T, Ito K, O'Kane CJ. 2010. Targeting expression to projection neurons that innervate specific mushroom body calyx and antennal lobe glomeruli in larval Drosophila. Gene Express Patterns 10:328–337.

Mathew D, Popescu A, Budnik V. 2003. Drosophila amphiphysin functions during synaptic Fasciclin II membrane cycling. J Neurosci 23:10710–10716.

Mauelshagen J. 1993. Neural correlates of olfactory learning paradigms in an identified neuron in the honeybee brain. J Neurophysiol 69:609–625.

McGuire SE, Deshazer M, Davis RL. 2005. Thirty years of olfactory learning and memory research in Drosophila melanogaster. Progr Neurobiol 76:328–347.

Menzel R. 2012. The honeybee as a model for understanding the basis of cognition. Nat Rev Neurosci 13:758–768.

Michels B, Chen YC, Saumweber T, Mishra D, Tanimoto H, Schmid B, Engmann O, Gerber B. 2011. Cellular site and molecular mode of synapsin action in associative learning. Learn Mem 18:332–344.

Mishra D, Miyamoto T, Rezenom YH, Broussard A, Yavuz A, Slone J, Russell DH, Amrein H. 2013. The molecular basis of sugar sensing in Drosophila larvae. Curr Biol 1466–1471.

Miyamoto T, Slone J, Song X, Amrein H. 2012. A fructose receptor functions as a nutrient sensor in the Drosophila brain. Cell 151:1113–1125.

Nassel DR, Wegener C. 2011. A comparative review of short and long neuropeptide F signaling in invertebrates: Any similarities to vertebrate neuropeptide Y signaling? Peptides 32:1335–1355.

Neckameyer WS, Woodrome S, Holt B, Mayer A. 2000. Dopamine and senescence in Drosophila melanogaster. Neurobiol Aging 21:145–152.

Neuser K, Husse J, Stock P, Gerber B. 2005. Appetitive olfactory learning in larvae: effects of repetition, reward strength, age, gender, assay type and memory span. Anim Behav 69:891–898.

Nicolai LJ, Ramaekers A, Raemaekers T, Drozdzecki A, Mauss AS, Yan J, Landgraf M, Annaert W, Hassan BA. 2010. Genetically encoded dendritic marker sheds light on neuronal connectivity in Drosophila. Proc Natl Acad Sci U S A 107:20553–20558.

Ohyama T, Schneider-Mizell CM, Fetter RD, Aleman JV, Franconville R, Rivera-Alba M, Mensh BD, Branson KM, Simpson JH, Truman JW, Cardona A, Zlatic M. 2015. A multilevel multimodal circuit enhances action selection in Drosophila. Nature 520:633–639.

Okada R, Rybak J, Manz G, Menzel R. 2007. Learning-related plasticity in PE1 and other mushroom body-extrinsic neurons in the honeybee brain. J Neurosci 27:11736–11747.

Oppliger FY, P MG, Vlimant M. 2000. Neurophysiological and behavioural evidence for an olfactory function for the dorsal organ and a gustatory one for the terminal organ in Drosophila melanogaster larvae. J Insect Physiol 46: 135–144.

Pauls D, Selcho M, Gendre N, Stocker RF, Thum AS. 2010. Drosophila larvae establish appetitive olfactory memories via mushroom body neurons of embryonic origin. J Neurosci 30:10655–10666.

Pauls D, von Essen A, Lyutova R, van Giesen L, Rosner R, Wegener C, Sprecher SG. 2015. Potency of transgenic effectors for neurogenetic manipulation in Drosophila larvae. Genetics 199:25–37.

Pech U, Pooryasin A, Birman S, Fiala A. 2013. Localization of the contacts between Kenyon cells and aminergic neurons in the Drosophila melanogaster brain using splitGFP reconstitution. J Comp Neurol.

Penzlin H. 1985. Stomatogastric nervous system. Compr Insect Physiol Biochem Pharmacol 5:371–406.

Python F, Stocker RF. 2002. Adult-like complexity of the larval antennal lobe of D. melanogaster despite markedly low numbers of odorant receptor neurons. J Comp Neurol 445:374–387.

Ramaekers A, Magnenat E, Marin EC, Gendre N, Jefferis GS, Luo L, Stocker RF. 2005. Glomerular maps without cellular redundancy at successive levels of the Drosophila larval olfactory circuit. Curr Biol 15:982–992.

Rescorla RA, Wagner AR. 1972. A theory of Pavlovian conditioning: Variations in the effectiveness of reinforcement and nonreinforcement. In: Black AH, Prokasy WF, editors. Classical conditioning II. New York: Appleton-Century-Crofts. p 64–99.

Rohwedder A, Pfitzenmaier JE, Ramsperger N, Apostolopoulou AA, Widmann A, Thum AS. 2012. Nutritional value-dependent and nutritional value-independent effects on Drosophila melanogaster larval behavior. Chem Senses 37:711–721.

Rotzinger S, Lovejoy DA, Tan LA. 2010. Behavioral effects of neuropeptides in rodent models of depression and anxiety. Peptides 31:736–756.

Scherer S, Stocker RF, Gerber B. 2003. Olfactory learning in individually assayed Drosophila larvae. Learn Mem 10: 217–225.

Schipanski A, Yarali A, Niewalda T, Gerber B. 2008. Behavioral analyses of sugar processing in choice, feeding, and learning in larval Drosophila. Chem Senses 33:563–573.

Schleyer M, Saumweber T, Nahrendorf W, Fischer B, von Alpen D, Pauls D, Thum A, Gerber B. 2011. A behavior-based circuit model of how outcome expectations organize learned behavior in larval Drosophila. Learn Mem 18: 639–653.

Schoofs A, Huckesfeld S, Surendran S, Pankratz MJ. 2014. Serotonergic pathways in the Drosophila larval enteric nervous system. J Insect Physiol 69:118–125.

Schroll C, Riemensperger T, Bucher D, Ehmer J, Voller T, Erbguth K, Gerber B, Hendel T, Nagel G, Buchner E, Fiala A. 2006. Light-induced activation of distinct modulatory neurons triggers appetitive or aversive learning in Drosophila larvae. Curr Biol 16:1741–1747.

Schwaerzel M, Monastirioti M, Scholz H, Friggi-Grelin F, Birman S, Heisenberg M. 2003. Dopamine and octopamine differentiate between aversive and appetitive olfactory memories in Drosophila. J Neurosci 23:10495–10502.

Selcho M, Pauls D, Han KA, Stocker RF, Thum AS. 2009. The role of dopamine in Drosophila larval classical olfactory conditioning. PLoS One 4:e5897.

Selcho M, Pauls D, El Jundi B, Stocker RF, Thum AS. 2012. The role of octopamine and tyramine in Drosophila larval locomotion. J Comp Neurol 520:3764–3785.

Selcho M, Pauls D, Huser A, Stocker RF, Thum AS. 2014. Characterization of the octopaminergic and tyraminergic neurons in the central brain of Drosophila larvae. J Comp Neurol 522:3485–3500.

Shen P, Cai HN. 2001. Drosophila neuropeptide F mediates integration of chemosensory stimulation and conditioning of the nervous system by food. J Neurobiol 47:16–25.

Shohat-Ophir G, Kaun KR, Azanchi R, Mohammed H, Heberlein U. 2012. Sexual deprivation increases ethanol intake in Drosophila. Science 335:1351–1355.

Singh RN, Singh K. 1984. Fine structure of the sensory organs of Drosophila melanogaster Meigen larva (Diptera: Drosophilidae). Int J Insect Morphol Embryol 13:255–273.

Spiess R, Schoofs A, Heinzel HG. 2008. Anatomy of the stomatogastric nervous system associated with the foregut

http://doc.rero.ch

in Drosophila melanogaster and Calliphora vicina third instar larvae. J Morphol 269:272–282.

Stewart S, Koh TW, Ghosh AC, Carlson JR. 2015. Candidate ionotropic taste receptors in the Drosophila larva. Proc Natl Acad Sci U S A 112:4195–4201.

Takagawa K, Salvaterra P. 1996. Analysis of choline acetyltransferase protein in temperature sensitive mutant flies using newly generated monoclonal antibody. Neurosci Res 24:237–243.

Thum AS, Knapek S, Rister J, Dierichs-Schmitt E, Heisenberg M, Tanimoto H. 2006. Differential potencies of effector genes in adult Drosophila. J Comp Neurol 498:194–203.

Thum AS, Leisibach B, Gendre N, Selcho M, Stocker RF. 2011. Diversity, variability, and subesophageal connectivity of antennal lobe neurons in D. melanogaster larvae. J Comp Neurol 519:3415–3432.

Tomer R, Denes AS, Tessmar-Raible K, Arendt D. 2010. Profiling by image registration reveals common origin of annelid mushroom bodies and vertebrate pallium. Cell 142:800–809.

Van Wielendaele P, Dillen S, Zels S, Badisco L, Vanden Broeck J. 2013. Regulation of feeding by Neuropeptide F in the desert locust, Schistocerca gregaria. Insect Biochem Mol Biol 43:102–114.

Vogelstein JT, Park Y, Ohyama T, Kerr RA, Truman JW, Priebe CE, Zlatic M. 2014. Discovery of brainwide neural-behavioral maps via multiscale unsupervised structure learning. Science 344:386–392.

von Philipsborn AC, Liu T, Yu JY, Masser C, Bidaye SS, Dickson BJ. 2011. Neuronal control of Drosophila courtship song. Neuron 69:509–522.

Wang Y, Pu Y, Shen P. 2013. Neuropeptide-gated perception of appetitive olfactory inputs in Drosophila larvae. Cell Rep 3:820–830.

Wen T, Parrish CA, Xu D, Wu Q, Shen P. 2005. Drosophila neuropeptide F and its receptor, NPFR1, define a signaling pathway that acutely modulates alcohol sensitivity. Proc Natl Acad Sci U S A 102:2141–2146.

White K, Steller H. 1995. The control of apoptosis in Drosophila. Trends Cell Biol 5:74–78.

White K, Grether ME, Abrams JM, Young L, Farrell K, Steller H. 1994. Genetic control of programmed cell death in Drosophila. Science 264:677–683.

White K, Tahaoglu E, Steller H. 1996. Cell killing by the Drosophila gene reaper. Science 271:805–807.

Williams G, Bing C, Cai XJ, Harrold JA, King PJ, Liu XH. 2001. The hypothalamus and the control of energy homeostasis: different circuits, different purposes. Physiol Behav 74:683–701.

Wong AM, Wang JW, Axel R. 2002. Spatial representation of the glomerular map in the Drosophila protocerebrum. Cell 109:229–241.

Wright GA, Mustard JA, Simcock NK, Ross-Taylor AA, McNicholas LD, Popescu A, Marion-Poll F. 2010. Parallel reinforcement pathways for conditioned food aversions in the honeybee. Curr Biol 20:2234–2240.

Wu Q, Wen T, Lee G, Park JH, Cai HN, Shen P. 2003. Developmental control of foraging and social behavior by the Drosophila neuropeptide Y-like system. Neuron 39:147–161.

Wu Q, Zhang Y, Xu J, Shen P. 2005a. Regulation of hunger-driven behaviors by neural ribosomal S6 kinase in Drosophila. Proc Natl Acad Sci U S A 102:13289–13294.

Wu Q, Zhao Z, Shen P. 2005d. Regulation of aversion to noxious food by Drosophila neuropeptide Y- and insulin-like systems. Nat Neurosci 8:1350–1355.

Xu J, Sornborger AT, Lee JK, Shen P. 2008. Drosophila TRPA channel modulates sugar-stimulated neural excitation, avoidance and social response. Nat Neurosci 11:676–682.

Xu J, Li M, Shen P. 2010. A G-protein-coupled neuropeptide Y-like receptor suppresses behavioral and sensory response to multiple stressful stimuli in Drosophila. J Neurosci 30:2504–2512.

Yamagata N, Ichinose T, Aso Y, Placais PY, Friedrich AB, Sima RJ, Preat T, Rubin GM, Tanimoto H. 2015. Distinct dopamine neurons mediate reward signals for short- and long-term memories. Proc Natl Acad Sci U S A 112:578–583.

Zimanyi IA, Fathi Z, Poindexter GS. 1998. Central control of feeding behavior by neuropeptide Y. Curr Pharm Design 4:349–366.

http://doc.rero.ch